Published in final edited form as:
Mol Microbiol. 2011 November ; 82(3): 679–697. doi:10.1111/j.1365-2958.2011.07845.x.

The coenzyme A disulfide reductase of *Borrelia burgdorferi* is important for rapid growth throughout the enzootic cycle and essential for infection of the mammalian host

Christian H. Eggers[1,*], **Melissa J. Caimano**[2], **Robert A. Malizia**[3], **Toru Kariu**[4], **Brian Cusack**[3], **Daniel C. Desrosiers**[2], **Karsten R.O. Hazlett**[2,†], **Al Claiborne**[5], **Utpal Pal**[4], and **Justin D. Radolf**[2,6,7]

[1]Department of Biomedical Sciences, Quinnipiac University, Hamden, CT 06518

[2]Department of Medicine, University of Connecticut Health Center, Farmington, CT 06030

[3]Department of Biology, Quinnipiac University, Hamden, CT 06518

[4]Department of Veterinary Medicine, University of Maryland, College Park, MD 20742

[5]Center for Structural Biology, Wake Forest School of Medicine, Winston-Salem, North Carolina 27157

[6]Department of Pediatrics, University of Connecticut Health Center, Farmington, CT 06030

[7]Department of Genetics and Developmental Biology, University of Connecticut Health Center, Farmington, CT 06030

Summary

In a microarray analysis of the RpoS regulon in mammalian host-adapted *Borrelia burgdorferi*, *bb0728* (*cdr*) was found to be dually-transcribed by the sigma factors σ^{70} and RpoS. The *cdr* gene encodes a coenzyme A disulfide reductase (CoADR) that reduces CoA-disulfides to CoA in an NADH-dependent manner. Based on the abundance of CoA in *B. burgdorferi* and the biochemistry of the enzyme, CoADR has been proposed to play a role in the spirochete's response to reactive oxygen species (ROS). To better understand the physiologic function(s) of *Bb* CoADR, we generated a *B. burgdorferi* mutant in which the *cdr* gene was disrupted. RT-PCR and 5′-RACE analysis revealed that *cdr* and *bb0729* are co-transcribed from a single transcriptional start site upstream of the *bb0729* coding sequence; a shuttle vector containing the *bb0729-cdr* operon and upstream promoter element was used to complement the *cdr* mutant. Although the mutant was no more sensitive to hydrogen peroxide than its parent, it did exhibit increased sensitivity to high concentrations of *t* -butyl-hydroperoxide, an oxidizing compound that damages spirochetal membranes. Characterization of the mutant during standard (15% oxygen, 6% CO_2) and anaerobic (<1% O_2, 9–13% CO_2) cultivation at 37°C revealed a growth defect under both conditions that was particularly striking during anaerobiosis. The mutant was avirulent by needle inoculation and showed decreased survival in feeding nymphs, but displayed no survival defect in unfed flat nymphs. Based on these results, we propose that *Bb* CoADR is necessary to maintain optimal redox ratios for CoA/CoA-disulfide and NAD^+/NADH during periods of rapid replication throughout the enzootic cycle, to support thiol-disulfide homeostasis, and to indirectly protect the spirochete against peroxide-mediated membrane damage; one or more of these functions are essential for infection of the mammalian host by *B. burgdorferi*.

[*] To whom correspondence should be addressed: Christian H. Eggers, Quinnipiac University, 275 Mount Carmel Ave, EC-BMS, Hamden, CT 06518-1908, Phone/fax: (203) 582-3767/ (203) 582-5317, Christian.eggers@quinnipiac.edu.
[†]Present address: Center for Immunology and Microbial Disease, Albany Medical College, Albany, NY 12208

Keywords

RpoS; CoADR; Lyme disease

Introduction

Borrelia burgdorferi, the causative agent of Lyme disease, persists in an enzootic cycle involving a tick vector and a vertebrate host, usually a rodent(Lane *et al*., 1991; Steere *et al*., 2004; Tilly *et al*., 2008). As the spirochete transitions between these two distinct host milieus, it must sense and adjust to changes in ambient temperature, oxygen tension, availability of carbon sources and other nutrients, and the presence of mammalian immune factors (Seshu and Skare, 2000; Tilly *et al*., 2001; Anguita *et al*., 2003; Pal and Fikrig, 2003; Seshu *et al*., 2004; Boylan *et al*., 2006; Dunham-Ems *et al*., 2009; Xu *et al*., 2010). The sigma factor RpoS is critical to the adaptations made by*B. burgdorferi* within feeding nymphs and the mammalian host, controlling the reciprocal up-regulation of genes necessary for the establishment of infection and the down-regulation of genes required within the vector (Hubner *et al*., 2001; Caimano *et al*., 2004; Caimano *et al*., 2005; Caimano *et al*., 2007; Ouyang *et al*., 2008; Ouyang *et al*., 2009). In a microarray analysis of the RpoSregulonin mammalian host-adapted spirochetes, we identified a small subset of genes that can be dually-transcribed bythe housekeeping sigma factor σ^{70} and the alternate sigma factor RpoS(Caimano *et al*., 2007). Among these is*bb0728* (*cdr*), which encodes a Coenzyme A disulfide reductase (CoADR) (Boylan *et al*., 2006; Caimano *et al*., 2007). First identified and characterized in *Staphylococcus aureus* (delCardayre and Davies, 1998; delCardayre *et al*., 1998),CoADRs subsequently have been annotated in the genomes of a number of organisms and biochemically characterized in *S. aureus*, *Bacillus anthracis*, *B. burgdorferi*, and *Pyrococcus horikoshii* (delCardayre and Davies, 1998; delCardayre *et al*., 1998; Harris *et al*., 2005; Hummel *et al*., 2005; Boylan *et al*., 2006; Mallett *et al*., 2006; Wallen *et al*., 2008). These enzymes reduce CoA-disulfides to CoA in an NAD(P)H-dependent manner in which the specificity for a particular pyridine nucleotide is dependent upon the organism(Wallen *et al*., 2008); the *B. burgdorferi* CoADR (*Bb* CoADR) utilizes NADH exclusively (Boylan *et al*., 2006). Interestingly, *cdr* is one of the few genes identified in the RpoS regulon encoding a protein with a predicted metabolic function(Caimano *et al*., 2007).

Pathogens grown in an aerobic environment must deal with the reactive oxygen species (ROS) generated both intracellularly and extracellularly as a major component of the mammalian innate immune defense against invading pathogens(Cabiscol *et al*., 2000; Imlay, 2003; Imlay, 2008; Sorci and Faivre, 2009).In addition to other damaging activities, ROS can cause inappropriate disulfide bond formation, inactivating protein function, and damaging or killing a cell (Imlay, 2002; Sevier and Kaiser, 2002; Kadokura *et al*., 2003). To combat this threat, organisms maintain abundant low-molecular weight thiols that function with specific Flavoprotein Disulfide Reductases (FDRs) and Thioredoxin Fold Proteins (TFPs) to sustain thiol-disulfide homeostasis(Holmgren, 1989; Carmel-Harel and Storz, 2000a; Holmgren *et al*., 2005; Imlay, 2008). Eukaryota and many Gram negative bacteria utilize glutathione and thioredoxin for this purpose (Holmgren, 1989; Carmel-Harel and Storz, 2000b; Holmgren *et al*., 2005). Gram positive bacteria and other more distantly related prokaryotes maintain pools of alternative low molecular weight thiols such as mycothiols(Newton *et al*., 1996; Newton *et al*., 2008), bacillithiols(Newton *et al*., 2009; Gaballa *et al*., 2010) or CoA(Newton *et al*., 1996; Hummel *et al*., 2005; Boylan *et al*., 2006; Nicely *et al*., 2007).*B. burgdorferi* encodes thioredoxin (Trx; *bb0061*) and a thioredoxin reductase (TrxB; *bb0515*) (Fraser *et al*., 1997) that is predicted to be NADPH-dependent, but the most abundant low-molecular weight thiol in the spirochete is CoA, which is found

almost entirely in the reduced form (CoASH)(Boylan *et al*., 2006). This suggests the involvement of CoADR in the maintenance of the cell's thiol/disulfide balance(delCardayre and Davies, 1998; delCardayre *et al*., 1998; Harris *et al*., 2005; Boylan *et al*., 2006; Wallen *et al*., 2008).Boylan, *et al*. (2006)also have reported that CoASH can directly reduce hydrogen peroxide(H_2O_2) *in vitro* ; the CoASH in the assay was regenerated by the addition of NADH and *Bb* CoADR. Direct involvement in the detoxification of peroxides has not previously been reported for CoA or CoADRs.

Given *B. burgdorferi* 'ssmall genome and limited biosynthetic capabilities, one also would anticipate an important role for *Bb* CoADR in intermediary metabolism(Gherardini *et al*., 2010). *Bb* CoADR is one of the few enzymes identified in the spirochete capable of regenerating the NAD^+ required for glycolysis, theorganism's sole means of energy production (Fraser *et al*., 1997). Additionally, CoA is a ubiquitous cofactor with an essential role as one of the predominant acyl group carriers in the intermediary metabolism of all organisms (Jackowski, 1996; Wolfe, 2005). Although the spirochete does not utilize acetyl-CoA for oxidative phosphorylation, it does require this molecule for a number of important anabolic pathways, including biosynthesis of phospholipids, glycolipids, lipoproteins and peptidoglycan for the maintenance and remodeling of its cell envelope (Fraser *et al*., 1997; Gherardini *et al*., 2010; Xu *et al*., 2010). *B. burgdorferi* lacks the common pathways (e.g., the AMP-forming acetyl-CoA synthetase [AMP-ACS] pathway, β-oxidationof fatty acids, and degradation of certain amino acids) for the production of acetyl-CoA (Fraser *et al*., 1997; Xu *et al*., 2010); its sole source of this essential compound appears to be synthesis from acetate and CoA via the Ack-Pta (acetate kinase-phosphate acetyltransferase) pathway (Xu *et al*., 2010; Sze and Li, 2011). The reduction of CoA disulfides by *Bb* CoADR would ensure adequate levels of CoASH for the production of acetyl-CoA, particularly during times of stress or increased replication, with the added bonus of yielding NAD^+ for energy generation.

The only previously published study of *Bb*CoADR was a biochemical analysis using recombinant enzyme(Boylan *et al*., 2006). To elucidate the physiological function of *Bb* CoADR, we generated a *B. burgdorferi* mutant in which the *cdr* gene was disrupted. Characterization of the mutant during standard (15% O_2, 5% CO_2) and anaerobic (<1% O_2, 9–13% CO_2)cultivation revealed a growth advantage under both conditions that, surprisingly, was particularly striking during anaerobiasis. In contrast to the prediction of (Boylan*et al*. (2006), the mutant was no more sensitive to hydrogen peroxide (H_2O_2) than its parent; it was, however, more sensitive to high concentrations of *t* -butyl-hydroperoxide, an oxidizing compound that damages spirochetal membranes(Boylan *et al*., 2008; Boylan and Gherardini, 2008).The mutant was avirulent by needle inoculation and showed diminished survival in feeding nymphs but no survival defect in flat nymphs. Based on these results, we propose that *Bb* CoADR is required to maintain optimal redox ratios for CoA/CoA-disulfide and NAD^+/NADH during periods of rapid replication, to support thiol-disulfide homeostasis, and to indirectly protect the spirochete against peroxide-mediated membrane damage; one or more of these functions are essential for infection of the mammalian host by *B. burgdorferi*.

Results

Predicted structure and bioinformatics of *Bb*CoADR

CoADR, along with NADH oxidase (Nox) and NADH peroxidase (Npx), represent the *P*eroxidase-*O*xidase-*R*eductase (POR) subgroup of the *F*lavoprotein *D*isulfide *R*eductase (FDR) family; in addition to the POR subgroup, the FDR family includes, among others, glutathione reductase (GR; DSR subgroup) and thioredoxin reductase (TrxR; AHR subgroup) (Argyrou and Blanchard, 2004; Ojha *et al*., 2007). Bacterial CoADR enzymes

have been well-described in *S. aureus*, *B. burgdorferi*, and*B. anthracis* (delCardayre and Davies, 1998; delCardayre *et al*., 1998; Boylan *et al*., 2006; Mallett *et al*., 2006; Wallen *et al*., 2008; Wallen *et al*., 2009). The crystal structures for oxidized *Sa* CoADR and *Ba* CoADR and for the reduced NADH and NADPH complexes of *Ba* CoADR have been reported previously (Mallett *et al*., 2006; Wallen *et al*., 2008; Wallen *et al*., 2009). Using the coordinates of the *Ba* CoADR-NADH complex, we generated a homology model for the *Bb* CoADR-NADH complex (Figure 1); *Ba* CoADR is 39% identical (63% similar) to *Bb* CoADR. Figure 1A shows the reduced *Bb* CoADR monomer with bound NADH, FAD and the CoASH product. The NADH, CoASH, and FAD are brought together within the predicted *Bb* CoADR active site formed, in part, by a cysteine residue (Cys42) from one polypeptide and two tyrosine residues (Tyr366′ and Tyr424′) from the second (Figure 1B). One functional distinction between the well-characterized bacterial CoADRs involves the pyridine nucleotide specificity: *Sa* CoADR has a preference for NADPH, *Ba* CoADR exhibits dual NAD(P)H specificity, and *Bb* CoADR preferentially utilizes NADH (delCardayre and Davies, 1998; delCardayre *et al*., 1998; Boylan *et al*., 2006; Wallen *et al*., 2008).Preference for a particular pyridine nucleotide can be indicative of an enzyme's role in the cell; enzymes that are NAD(H)-dependent are more likely involved in the regeneration of oxidized pyridine nucleotides for glycolysis (Argyrou and Blanchard, 2004; Harris *et al*., 2005; Ying, 2006; Ying, 2008). Of the CoADRs thus far examined, only *Bb* CoADR selectively uses NADH(delCardayre and Davies, 1998; delCardayre *et al*., 1998; Gouet *et al*., 1999; Harris *et al*., 2005; Boylan *et al*., 2006; Mallett *et al*., 2006; Wallen *et al*., 2008).To determine whether *Bb* CoADR is unusual among CoADRs in its preference for NADH or whether NADH-selectivity is a hallmark of Gram negative bacteria and/or spirochetes, we analyzed the NAD(P)H-binding motifs of CoADR orthologs annotated in 17 distinct species, including spirochetes (from the genus *Brachyspira*) and both Gram-negative γ-and δ-proteobacteria (Figure 1C). NADH-selectivity of members of the FDR family depends largely upon the contribution of a Gly residue at position 162 and either a Glu or Asp residue at position 180 (positions given relative to *Ba* CoADR for clarity)(Karplus and Schulz, 1989; Stehle *et al*., 1993; Wallen *et al*., 2008) (Figure 1C).Based on sequence data, and in the absence of structural and functional data, we predict that, in addition to the *Bb* CoADR, four of the analyzed CoADRs (from three *Aeromonas* species and *Ferrimonas balearica*) also selectively utilize NADH. The rest have binding motifs consistent either with NADPH-selectivity (n = 3) or the ability to use both pyridine nucleotides (n = 10) (Figure 1C).

Construction of a *cdr* mutant in *B. burgdorferi*

To investigate the function of *Bb* CoADR, we generated a *cdr* null mutant in c162, a virulent clone of *B. burgdorferi* strain 297 (Steere *et al*., 1984) (Table 1). For this purpose, we cloned the erythromycin-resistance gene (*ermC*) from pGK12 (Kok *et al*., 1984; Sartakova *et al*., 2000) into two native *Eco*RI sites 197 and 1203 nucleotides from the 5′ end of the 1330-nucleotide *cdr* open reading frame (Fraser *et al*., 1997) (Figure 2). Removal of this fragment leaves 44 N-terminal amino acids (10% of the 444 total) that include part of the FAD-BD1 domain containing the active site Cys42, but eliminates the NADH-binding domain, FAD-BD2, and the Interface domain including Tyr366(Mallett *et al*., 2006; Wallen *et al*., 2008; Wallen *et al*., 2009) (Figures 1A and 1B). Thus, this mutation is expected to completely abrogate the activity of *Bb* CoADR. To select the mutant, c162 cells electroporated with the *cdr* -knockout construct were split into two aliquots and grown in the presence of erythromycin at 37°C under standard (15% O_2, 6% CO_2) or anaerobic (<1% O_2, 9–13% CO_2) conditions. Both conditions were used in anticipation of the possibility that the mutation would render the cells sensitive to oxygen; however, erythromycin-resistant clones with the appropriate insertion (not shown) were recovered using both conditions. One clone

recovered under anaerobic conditions, designated c309 (Table 1), was selected for further study.

Promoter identification and generation of a complemented clone of the *cdr* mutant

When the sequence of *B. burgdorferi* strain B31 was released (Fraser *et al*., 1997), the *cdr* gene was predicted to form a two-gene operon with *bb0729* (Figure 3A); *bb0729* has been annotated as encoding a dicarboxylate amino acid (Glu) transporter(Fraser *et al*., 1997), but the predicted gene product is 50% identical with TcyP, a Na^+/cystine symporter of *B. subtilis* (Burguiere *et al*., 2004; Overbeek *et al*., 2005). As shown in Figure 3B, amplification of *B. burgdorferi* cDNA using primers that lie within *bb0729* and *bb0728* (Table 2) confirmed that these two genes are co-transcribed. To generate a complement ofc309in which the *cdr* gene was re-introduced under the control of its own promoter, we next had to identify the region controlling *cdr* expression. 5′-RACE using primers internal to either *cdr* (primers 16–18) or *bb0729* (primers 18–21) (Figure 3A and Table 2) revealed a single strong transcriptional start at position −9 relative to the translational start of *bb0729* ; this is immediately upstream of the predicted ribosomal binding site for *bb0729* (illustrated in Figure 3A). In contrast, amplification upstream of the *cdr* open reading frame yielded no product. A comparison of the ‘extended −10’ and −35 regions of the *bb0729* promoter with a consensus sequence previously identified for RpoS-dependent genes (Caimano *et al*., 2007) reveals that the −35 region sequence (TTAAGT) differs by two nucleotides while the ‘extended −10 region’ (TGCACTAAGCT) differs by four.

Boylan *et al*., 2006; reported that the transcription factor BosR (BB0647) enhanced expression of *cdr* by binding somewhere within a 225-bp region upstream of *bb0729*. While two potential consensus sequences for BosR binding have been identified, neither element was found within the region directly upstream of *bb0729* (Katona *et al*., 2004; Ouyang *et al*., 2011). Nevertheless, to ensure that any potential regulatory elements proximal to the promoter were included in the construct used for complementation of the *cdr* mutant, we amplified the entire *bb0729-cdr* operon, including the 500-bp upstream region to generate the complementing plasmid pCE1735. All transformants selected contained pCE1735 but lacked the endogenous *B. burgdorferi* plasmid lp28-1; after multiple unsuccessful attempts to recover a complemented clone with a complete plasmid complement, we selected one lacking lp28-1 (c1655, Table 1) for further study.

Transcriptional analysis of *cdr* during *in vitro* growth

To determine whether *cdr* expression is sensitive to changes in oxygen tension during *in vitro* growth, qRT-PCR was performed on RNAs harvested from the wild-type clone, c162, cultured at 37°C under both standard (15% oxygen, 6% CO_2) and anaerobic (<1% O_2, 9–13% CO_2) growth conditions; c309 (mut) and c1655 (ct) were included in these analyses to assess levels of *cdr* expression in the mutant and complement. As shown in Figure 4, while copy numbers of *cdr* transcripts are quite low, c162 produced significantly more transcript ($P < 0.05$) under standard growth conditions than when grown anaerobically (Figure 4). As expected, no transcript was detected in c309 under either condition. While transcript levels in c162and c1655were virtually identical under anaerobic conditions, transcript levels in c162 were approximately twice those in c1655 under standard conditions. This difference under standard conditions may suggest regulatory elements found within the context of the native gene that are not present in the complementing construct, however the difference did not affect complementation of the *cdr* mutation (see below).

The role of *cdr* in defense against peroxide stress

Boylan *et al*., 2006;previously have proposed that CoADR protects the spirochete against H_2O_2based on their demonstration that CoA was able to reduce this oxidant *in vitro* in a

process that required CoADR activity to replenish the reduced CoA. To determine whether a *cdr* mutant is more sensitive to exogenous peroxide than the wild-type, c162, c309 (mut) and c1655 (ct) initially grown under standard conditions were exposed to concentrations of H_2O_2 from 0 to 10 mM (Figure 5A). Although both c162 and c309 showed modest sensitivity to exposure at 5 mM $H_2O_2$and none of the clones had measurable survival at 10 mM H_2O_2, we observed no significant difference in the sensitivity of c309 to H_2O_2-stress relative to c162 or c1655 at any concentration.

The primary targets of ROS in *B. burgdorferi* appear to be spirochetal membranes (Boylan *et al*., 2008; Boylan and Gherardini, 2008). To test whether a *cdr* mutant is more sensitive than the wild-type to membrane damage, c162, c309, and 1655 were exposed to 0 to 10 mM of *t* -butyl-hydroperoxide (Figure 5B), an oxidizing agent that has been demonstrated to initiate lipid peroxidation in *B. burgdorferi* outer membranes *in vitro* (Boylan *et al*., 2008; Boylan and Gherardini, 2008). At every concentration of *t* -butyl-hydroperoxide, the mutant appeared more sensitive to exposure than the wild-type; the difference between the two was significant at 5 mM ($P < 0.05$). This difference was due to the absence of the *cdr* gene, as the complement was not significantly more sensitive than the wild-type at any concentration.

Spirochetes lacking BbCoADR exhibit a growth defect under both aerobic and anaerobic conditions

Given the potential role(s) of CoADR in both intermediary metabolism and oxidative stress response, we wanted to determine if the *cdr* mutant exhibited a growth defect and, if so, whether it was influenced by the presence or absence of oxygen. Accordingly, c162 (wt), c309 (mut), and 1655 (ct) were grown at 37°C under standard or anaerobic conditions (Figure 6). c162 reached equivalent densities under both conditions, although it entered stationary phase approximately 48 hours later under anaerobic conditions (arrows in Figure 6). Under standard conditions, c309 exhibited a significant growth defect (Figure 6, left panel). By day 10, the last day on which growth was measured, the density of c309 plateaued at 70% of the final density of c162. The growth defect of c309 was even more severe under anaerobic conditions (Figure 6, right panel); the density of c309 at day 10 was only 8% that of the wild-type and complemented clones and did not rise appreciably by day 14 (not shown). Under both conditions, c162 and c1655 grew indistinguishably.

At 37°C *in vitro*, more than 50% of the expression of *cdr* is RpoS-dependent (Caimano *et al*., 2007). To determine if an *rpoS* -mutant exhibits the same *in vitro* growth defect as observed with the *cdr* mutant, we compared the growth of the *rpoS* -mutant c174 (Caimano *et al*., 2004; Eggers *et al*., 2004; Caimano *et al*., 2005)(Table 1) with that of its parent, c162, grown at 37°C under both standard and anaerobic conditions. In contrast to the *cdr* -mutant (Figure 6), the *rpoS* -mutant grew as well as the wild-type under both conditions (Figure 7). Thus, the RpoS-dependent component of *cdr* expression is not required for normal *in vitro* growth in BSK-II medium.

BbCoADR is required for infectivity in the murine model

To test the infectivity of the *cdr* mutant, we needle-inoculated two groups of five C3H/HeJ mice with 1×10^4spirochetes of either clone c162 (wt) or c309 (mut). Eight weeks post-inoculation, infection was assessed by serology and ear tissue biopsy. All of the mice infected with c162 developed a robust immune response to multiple borrelial antigens, whereas the mice inoculated with c309 failed to seroconvert, developing antibodies to only one major 20-kDa band; this band was confirmed to be OspC by blotting against purified OspC protein (data not shown and Table 3). All mice infected with c162 also were culture-positive, while spirochetes were not recovered from mice inoculated with c309 (Table 3).

To confirm that the avirulence of c309 was due to the lack of CoADR, we inoculated SCID mice with 1×10^4spirochetes of clones c162, c309, or the complement, c1655. SCID mice were used because c1655 lacks 1p28-1, which is required for survival in immunocompetent mice (Labandeira-Rey and Skare, 2001; McDowell *et al*., 2002; Labandeira-Rey *et al*., 2003; Lawrenz *et al*., 2004). Four weeks post-inoculation, infection was assessed by culture of ear punch biopsies. As presented in Table 3, all mice inoculated with c162 or c1655 were culture-positive, whereas no spirochetes were isolated from c309. Additionally, all mice infected with c162 and nine of the ten mice inoculated with c1655 also exhibited visible swelling in the rear ankle joints, whereas none of those inoculated with c309 had visible swelling (Table 3 and data not shown).

Transcriptional profiling of *cdr* within ticks

The expression profile of *cdr* had previously been characterized *in vitro* at 23°C and 37°C and in dialysis membrane chambers (DMCs) implanted into the peritoneal cavity of rats (Caimano *et al*., 2007). Transcriptional analyses of spirochetes within ticks were next performed to gain insight into the contribution of the gene to spirochetal physiology during the tick phase of the enzootic cycle. qRT-PCR demonstrated that *cdr* is expressed in all three tick phases; of note, spirochetes in fed nymphs and larvae contain on average, more than twice as much *cdr* transcript as spirochetes in unfed nymphs (Figure 8A). RpoS is not expressed in fed larvae or unfed nymphs, but is induced during the nymphal blood meal (Caimano *et al*., 2007). To determine whether the increase in *cdr* transcript observed within the midguts of fed nymphs was due to transcription by RpoS, we immersion-fed nymphs with both c162 (wt) and c174 (*rpoS* mutant)(Policastro and Schwan, 2003; Mulay *et al*., 2009). After a brief rest period, these ticks were allowed to feed on uninfected mice. RNA was harvested from the midguts of engorged nymphs and *cdr* transcript was analyzed by qRT-PCR. As shown in Figure 8B, in fed nymphs, levels of *cdr* in the *rpoS* mutant are approximately 50% of those in the wild-type, confirming the partial RpoS-dependence of *cdr* expression under certain conditions (Caimano *et al*., 2007).

Loss of *cdr* affects survival of spirochete in fed, but not flat nymphs

To determine whether *Bb* CoADR is required within the midguts of flat and/or feeding nymphs, equivalent numbers of c162 (wt), c309 (mut), and c1655 (ct) (~10^4 spirochetes/tick) were microinjected into the midguts of *Ixodes scapularis* nymphs (Pal *et al*., 2004; Kariu *et al*., 2011). While immersion feeding can be used to generate large numbers of infected larvae or nymphs (Policastro and Schwan, 2003), for these experiments microinjection was used instead because the number of spirochetes delivered could be standardized, 100% infectivity could be ensured, and more rapid results could be acquired (Kariu *et al*., 2011). After a ten day rest period, spirochete burdens in unfed nymphs were assessed by qRT-PCR analysis of *B. burgdorferi flaB* mRNA and normalized against the tick β-actin gene as previously described (Zhang *et al*., 2009). The levels of *flaB* mRNA in unfed nymphs were virtually identical for all three clones (Figure 9A). During feeding, however, the numbers of the *cdr* mutant in the midgut of fed nymphs were significantly lower ($P < 0.05$) than those of either the wild-type or the complemented mutant (Figure 9B). These data indicated an inability of the *cdr* mutant to expand appropriately within the midgut. We also observed that equivalent numbers of SCID mice became infected after being fed on by nymphs colonized with either c162 or c1655; no SCID mice fed upon by nymphs colonized with c309 became infected (data not shown).

Discussion

Dissecting the functional role(s) of a borrelial enzyme that potentially contributes to the spirochete's oxidative stress response as well as intermediary metabolism is complicated by

the fact that both increased oxygen levels and signals to stimulate replication are delivered simultaneously within blood and during mammalian infection (Seshu and Skare, 2000; Tilly *et al*., 2001; Piesman *et al*., 2001; Zeidner *et al*., 2001; Anguita *et al*., 2003; Pal and Fikrig, 2003; Seshu *et al*., 2004; Boylan *et al*., 2006; Boylan *et al*., 2008; Dunham-Ems *et al*., 2009; Xu *et al*., 2010). Using a strategy combining *in vitro* and *in vivo* analyses, we have presented evidence supporting the conclusion that CoADR functions in both capacities to promote spirochetal fitness. In particular, our observation that the *cdr* mutant has a much greater growth impairment when cultivated *in vitro* anaerobically than with oxygen strongly implies a homeostatic role for CoADR independent of defense against ROS.

The enzymatic mechanisms *B. burgdorferi* employs to protect itself against different types of oxidative stress are poorly understood. *B. burgdorferi* encodes few homologues to proteins known to participate in the oxidative stress response of other bacteria (Fraser *et al*., 1997; Gherardini *et al*., 2010; Parsonage *et al*., 2010) (Table 4). In addition to CoADR, *B. burgdorferi* encodes only a single member of the TFP class (thioredoxin, Trx; *bb0061*), a thioredoxin reductase (TrxB; *bb0515*),a Dps/Dpr homologue (NapA; *bb0690*) and a superoxide dismutase (SodA; *bb0153*)(Fraser *et al*., 1997; Seshu *et al*., 2004; Boylan *et al*., 2006; Li *et al*., 2007; Esteve-Gassent *et al*., 2009; Parsonage *et al*., 2010). Conspicuous in their absence are peroxiredoxins, glutathione peroxidases, catalases, and both glutathione biosynthetic and glutaredoxin proteins(Fraser *et al*., 1997; Gherardini *et al*., 2010; Parsonage *et al*., 2010) (Table 4). Based on their *in vitro* biochemical activities, CoADRs have been proposed to be important for maintaining the intracellular thiol-disulfide ratio and possibly in protecting the cell from ROS (delCardayre and Davies, 1998; delCardayre *et al*., 1998; Argyrou and Blanchard, 2004; Harris *et al*., 2005; Boylan *et al*., 2006; Wallen *et al*., 2008). Consistent with this notion, the *B. burgdorferi cdr* mutant exhibited a growth defect under *in vitro* and *in vivo* conditions in which higher levels of ROS were more likely to be present (Imlay, 2003). Furthermore, we found that in wild-type *B. burgdorferi*, *cdr* was expressed more than three times higher under standard (aerobic) conditions than under anaerobic conditions, as would be expected for a gene encoding a protein involved in the defense against noxious oxidative molecules (Stanton *et al*., 1999; Cabiscol *et al*., 2000). Thus, it appears likely that CoA and CoADR function analogously to glutathione and GR in Eukaryota and most Gram negative bacteria to maintain an appropriate intracellular thiol/disulfide ratio(Holmgren, 1989; Carmel-Harel and Storz, 2000a; Boylan *et al*., 2006; Imlay, 2008). It is important to note, however, that while the biochemical mechanisms whereby glutathione and Grx maintain reduced disulfide bonds in cellular proteins are well understood (Holmgren, 1989; Carmel-Harel and Storz, 2000a), it is not known whether CoASH has a role in reducing disulfide bonds in *B. burgdorferi*, nor what the mechanism for this activity might be.

While CoADR may play a role in supporting intracellular thiol-disulfide homeostasis, the absence of this enzyme failed to render spirochetes more sensitive than the wild-type to high concentrations of H_2O_2. These results call into question the physiologic relevance of the *in vitro* observation that CoADR could participate in the detoxification of $H_2O_2$by reducing CoA-disulfides generated by the reaction of CoA with peroxide (Boylan *et al*., 2006). Membrane lipids are the primary target of ROS in *B. burgdorferi* (Boylan *et al*., 2008). The *cdr* mutant was more sensitive than the wild-type to high levels of *t* -butyl-hydroperoxide, an organic hydroperoxide known to initiate lipid peroxidation in *B. burgdorferi* membranes (Boylan *et al*., 2008; Boylan and Gherardini, 2008). The direct detoxification of organic hydroperoxides in bacteria is primarily catalyzed by peroxiredoxin TFPs distinct from the members of the FDR family that includes CoADR(Argyrou and Blanchard, 2004; Poole, 2005; Parsonage *et al*., 2008). In fact, *B. burgdorferi* contains no homologs to enzymes capable of detoxifying organic peroxides (Fraser *et al*., 1997; Parsonage *et al*., 2010). Thus, the greater sensitivity of the *cdr* mutant to exogenous *t* -butyl hydroperoxide most likely

reflects the requirement for the cytoplasmic CoADR to ensure an adequate pool of acetyl-CoA or acyl-CoA (via maintenance of optimal levels of intracellular CoA) for synthesis of the lipids, glycolipids, or lipoproteins needed for membrane repair following lipid peroxidation (Gherardini *et al*., 2010).

The likely contributions of CoADR to the metabolism of *B. burgdorferi* can be deduced from its known biochemistry (Boylan *et al*., 2006). In addition to making CoASH available for formation of acetyl-CoA, a precursor for many biosynthetic reactions (Fraser *et al*., 1997; Wolfe, 2005; Gherardini *et al*., 2010; Xu *et al*., 2010), CoADR also supplies the NAD^+ that is essential for substrate-level phosphorylation through glycolysis, the sole mechanism for ATP generation in *B. burgdorferi* (Fraser *et al*., 1997). Utilizing The SEED resource(Overbeek *et al*., 2005), we identified only a few *B. burgdorferi* proteins presumed or known to rely on NAD(H): glyceraldehyde-3-phosphate dehydrogenase (*bb0057*), lactate dehydrogenase (LDH) (*bb0087*), glycerol-3-phosphate dehydrogenase (*bb0368*),hydroxymethylglutaryl (HMG)-CoA reductase (*bb0685*), and CoADR. The other two members (Nox and Npx) of the POR subgroup of the FDR family also contribute to the obligatory role of NAD^+ in the strictly fermentative energy metabolism of *Streptococcus* and other lactic acid bacteria (Higuchi *et al*., 1999; Gibson *et al*., 2000).While *Bb* CoADR is the only CoADR thus far experimentally determined to have a preference for NADH, our bioinformatics analysis indicates the presence of several additional enzymes among the γ-proteobacteria that are predicted to be NADH-specific. In general, FDR enzymes that utilize NAD(H) are more likely involved in the regeneration of oxidized pyridine nucleotides for glycolysis, whereas those that are NADPH-dependent tend to be involved in the maintenance of thiol/disulfide homeostasis(Argyrou and Blanchard, 2004; Harris *et al*., 2005; Ying, 2006; Ying, 2008).

In contrast to the growth defect observed during anaerobiasis*in vitro*, we found that the *cdr* mutant did not exhibit a loss of viability when maintained within the anaerobic environment of the unfed tick midgut(Seshu *et al*., 2004) for ten days following rectal infusion. Spirochetes cultured anaerobically *in vitro* replicate exponentially, whereas they replicate minimally or not at all within the unfed midgut(Zeidner *et al*., 2001; Piesman *et al*., 2003). Thus, the metabolic requirements of the spirochetes in the unfed tick differ significantly from those of organisms grown in BSK-II medium in culture, further suggesting that the defect observed in spirochetes grown anaerobically *in vitro* could be due to metabolic deficiencies such as inadequate NAD^+ or CoASH. We also found that the *cdr* mutant exhibited a growth defect within the feeding nymph and within the mammalian host. Both are environments in which spirochetes encounter increased oxygen tensions and concentrations of ROS (Seshu *et al*., 2004; Boylan *et al*., 2006; Gherardini *et al*., 2010) but also in which they undergo marked replication (Piesman *et al*., 2001; Zeidner *et al*., 2001; Piesman *et al*., 2003; Hodzic *et al*., 2003; Dolan *et al*., 2004). We hypothesize that mutant spirochetes failed to thrive in both host environments at least in part because they were unable to generate sufficient energy and the precursors required to generate new cell envelopes.

Our results indicate that the metabolic importance of CoADR to *B. burgdorferi* is dependent upon the environment in which the spirochete is cultured. While we observed a defect with the *cdr* mutant grown under any condition with increased exposure to oxygen or increased replication requirements, only within the mammalian host did CoADR appear to be essential. Why is the *cdr* mutation not equally detrimental under all conditions? The different phenotypes observed with the *cdr* mutant in various environments may reflect the availability of differentially-expressed redundant metabolic pathways that enable the spirochete to overcome the lack of CoADR to varying extents. For example, although the thioredoxin-dependent reduction system has not been characterized in *B. burgdorferi*, it

presumably functions in the maintenance of the thiol/disulfide balance as in other systems (Holmgren, 1989; Holmgren, 2000; Carmel-Harel and Storz, 2000a; Holmgren *et al*., 2005); perhaps under certain conditions this pathway can partially complement the function(s) of CoADR; in other organisms with two disulfide reduction systems, single mutants are often not hypersensitive to oxidants because of partial overlap in those systems (Carmel-Harel and Storz, 2000a).

The ability of *B. burgdorferi* to use CoADR to fulfill roles in both thiol/disulfide homeostasis and intermediary metabolism is predicated on the idea that the spirochete can synthesize and maintain a large pool of CoA. While *de novo* biosynthesis of pantothenate (Pan) in *B. burgdorferi* from α-ketoisovalerate and aspartate is absent (*pan BCDE* genes in *E. coli*), *B. burgdorferi* encodes a putative Pan transporter (BB0814, PanF, Na^+/Pan symporter, Table 4)(Boylan *et al*., 2006; Gherardini *et al*., 2010); Pan is a precursor for CoA synthesis (Jackowski and Rock, 1981; Jackowski, 1996; Gherardini *et al*., 2010) and Gherardini and colleagues (Boylan *et al*., 2006; Gherardini *et al*., 2010) previously have proposed that the spirochete can synthesize CoA using Pan acquired from their environment. Based on bioinformatics, we also have identified a type III Pan kinase ortholog (PanK, BB0527; Table 4) for production of 4′-phosphopantothenate (Pan-4′-$P_!$). The use of a type III PanK allows for uncoupling of the kinase reaction from CoASH feedback inhibition(Nicely *et al*., 2007; Paige *et al*., 2008) and is consistent with the spirochete's dependence on CoA as the major low molecular weight thiol(Boylan *et al*., 2006).The spirochete also contains *coaBC*, *coaD*, and *coaE* loci predicted to encode proteins for conversion of Pan-4′-$P_!$ to CoASH(Boylan *et al*., 2006; Gherardini *et al*., 2010) (Table 4).Interestingly, the *coaD* (BB0702) locus is associated with a cluster that includes the *acpP* (BB0704) coding sequence; acyl carrier protein (AcpP) functions in fatty acid synthesis *via* the obligatory participation of the covalently bound 4′-phosphopantetheine cofactor derived from CoASH(Chan and Vogel, 2010; Gherardini *et al*., 2010). One other metabolite necessary for the synthesis of CoA is L-cysteine (Jackowski and Rock, 1981; Jackowski, 1996). *bb0729*, the upstream gene co-transcribed with *cdr*, has homology to the *Bacillus subtilis* TcyP protein (Overbeek *et al*., 2005), a Na+/cystine symporter(Burguiere *et al*., 2004) (Table 4); cystine is the oxidized form of L-cysteine. The genomic proximity of genes encoding TcyP homologs and CoADRs is found in other non-borrelial bacteria as well, including other pathogens such as *Clostridium difficile*. Given the potential relationship between cystine transport and CoA biosynthesis, the metabolic linkage between *Bb* CoADR and the product of *bb0729* warrants further investigation.

Our interest in *cdr* stemmed in part from our earlier finding that it is one of a small number of genes within the RpoSregulon that is dually-transcribed by σ^{70} and RpoS following temperature shift or cultivation within DMCs (Caimano *et al*., 2007). Two observations made herein have afforded additional insight into the biological context and rationale for dual transcription of the gene. First, we showed that *cdr* also is dually-transcribed during nymphal feeding, the stage in which RpoS-dependent gene expression begins. Thus, co-transcription of this operon is the rule when both RpoS-dependent and –independent gene expression are occurring. The ability of both sigma factors to control expression of the *bb0729-cdr* operon is explained by our finding that *cdr* and *bb0729* appear to be co-transcribed from a single hybrid promoter with consensus sequence elements consistent with both RpoS- and σ^{70}-dependent promoters (Caimano *et al*., 2007). Second, we found that transcription of *cdr* in feeding larvae, when RpoS is OFF, occurs at comparable levels to that in feeding nymphs. These results clearly imply that comparable levels of the enzyme are required when spirochetes are replicating rapidly regardless of whether RpoS is ON or OFF (Piesman *et al*., 2001; Zeidner *et al*., 2001; Piesman *et al*., 2003; Caimano *et al*., 2007). We find it intriguing that σ^{70} is capable of achieving full transcription of the gene in the absence of RpoS during larval acquisition but is unable to compensate for its loss during nymphal

feeding. This result suggests that another transcription factor either enhances σ^{70}-dependent replication within spirochetes found in larval ticks or represses σ^{70}-dependent replication within spirochetes found in feeding nymphs. Based (i) on data showing that BosR could bind upstream of the *bb0729-cdr* operon promoter and enhance transcription of *cdr* in an *E. coli* -based surrogate system (Boylan *et al*., 2006) and (ii) on the finding that a *bosR* mutant failed to regulate CoADR protein expression appropriately(Hyde *et al*., 2009), the Fur homolog BosR seems like a potential candidate transcription factor for *in vivo* regulation of *cdr* (Boylan *et al*., 2006; Hyde *et al*., 2009).Interestingly, however, reported consensus sequences identified for BosR-binding sites (Boylan *et al*., 2003; Katona *et al*., 2004; Ouyang *et al*., 2011)were not found directly upstream of the transcriptional start of the *bb0729-cdr* operon, and *cdr* was not identified as BosR-dependent in a recent microarray analysis of a *bosR* mutant (Ouyang *et al*., 2009). Thus, whether BosR directly regulates*cdr* transcription *in vivo* has yet to be determined.

If the spirochete can achieve transcript levels with σ^{70} sufficient for its metabolic needs in the larvae, why is *cdr* expression partially RpoS-dependent during the nymphal blood meal? The answer may lie in the interrelationship between the function and regulation of the RpoSregulon. RpoS-enhanced expression of *cdr* is not needed in the nutrient-rich BSK-II culture medium, however recent ongoing work suggests that RpoS-enhanced levels of CoADR are required in the feeding nymph or under nutrient-limiting conditions *in vitro* (Dunham-Ems &Radolf, unpublished data). While the link between RpoS and the CoADR is still under investigation, there is now a growing body of evidence that the physiological changes required to execute the spirochete's infectious program are intrinsically-linked to the Ack-Pta pathway for the synthesis of acetyl-CoA from acetate (Sanjuan *et al*., 2009; Xu *et al*., 2010; Karna *et al*., 2011; Sze and Li, 2011). In *B. burgdorferi*, AckA (BB0622) converts exogenously acquired acetate into acetyl-P, which is itself converted into acetyl-CoA by the enzyme Pta (BB0589) (Xu *et al*., 2010; Gherardini *et al*., 2010). Acetyl-P also has been shown to activate the response regulator, Rrp2, by phosphorylation(Xu *et al*., 2010). Phosphorylated Rrp2 acts in concert with RpoN and BosR to transcribe RpoS(Hubner *et al*., 2001; Yang *et al*., 2003; Caimano *et al*., 2004; Fisher *et al*., 2005; Ouyang *et al*., 2008; Boardman *et al*., 2008; Hyde *et al*., 2009; Ouyang *et al*., 2009; Blevins *et al*., 2009; Mulay *et al*., 2009; Xu *et al*., 2010; Ouyang *et al*., 2011). Thus, an increase in acetate, such as might occur with an influx of blood, increases acetyl-P, which ultimately activates the expression of RpoS-dependent virulence factors, including CoADR. Abundant CoADR would ensure higher levels of CoASH that could be used in the formation of acetyl-CoA. Acetate, CoA, and acetyl~P levels would work synergistically to modulate RpoS expression and, ultimately, the expression of RpoS-dependent virulence related genes.

Experimental Procedures

Computer modeling

The three-dimensional model of *Bb* CoADRwas generated by the SWISS-MODEL server based on the structure of the reduced*Bacillus anthracis* CoADR (*Ba* CoADR)-NADH complex [PDB code: 3CGD(Wallen *et al*., 2008)](Arnold *et al*., 2006; Bordoli *et al*., 2009). PyMOL (Schrödinger, New York, NY) was used to generate the structural graphics.

Bacterial strains and culture conditions

All PCR primers used in this study are listed in Table 2.Routine cloning and plasmid propagation were performed using *Eschericia coli* strain Top10 (Invitrogen). All strains were maintained at 37°C in Luria-Bertani broth (LB) (1% Tryptone, 0.5% yeast extract, 1% NaCl) with the appropriate antibiotic. Preparation and transformation of chemically-competent *E. coli* were performed as described previously (Ausubel *et al*., 1997). Solid

phase selection was performed on LB agar plates (LB with 1.5% agar) supplemented with the appropriate antibiotic.

All experiments with *B. burgdorferi* were performed using c162 (Caimano *et al*., 2007), a virulent clone of *B. burgdorferi* strain 297 (Steere *et al*., 1984), or its derivatives: c174 (*rpoS::ermC*) (Caimano *et al*., 2004; Eggers *et al*., 2004; Caimano *et al*., 2005), c309 (*cdr::ermC*), or c1655 (c309+pCE1735) (Table 1). Spirochetes were routinely cultivated in modified Barbour-Stoenner-Kelly medium supplemented with 6% rabbit serum (Pel-Freez Biologicals, Rogers, AK)(BSK-II)(Samuels, 1995); when appropriate, selection and maintenance of *B. burgdorferi* clones was performed in media supplemented with 0.06 μg ml^{-1} erythromycin (c309 and c174), 400 μg ml^{-1} kanamycin (JH300) or 0.06 μg ml^{-1} erythromycin and 400 μg ml^{-1} kanamycin (c1655). For routine cultivation, spirochetes were maintained at 33°C in liquid culture in tightly-capped containers with a low void volume [micro aerobic(Seshu *et al*., 2004)]. For experiments comparing growth in the presence or absence of oxygen (see below), *B. burgdorferi* was grown at 37°C in containers with loose lids either in a chamber with an enhanced CO_2 environment (15% O_2, 6% CO_2) generated by the addition of an enhanced CO_2 packet (GasPak™ EZ CO_2 Container System; Becton-Dickinson) (termed 'standard' conditions) or in a chamber with an anaerobic environment (<1% O_2, 9–13% CO_2) created by the inclusion of an anaerobic packet (BBL GasPak Plus Anaerobic System; Becton-Dickinson); anaerobiasis was monitored by the addition of BBL Dry Anaerobic Indicator Strips (Becton-Dickinson). For all experiments, spirochetes were passaged no more than three times before experimental manipulations were performed; plasmid contents were monitored by PCR as described previously (Eggers *et al*., 2002).

Generation of a *bb0728 (cdr)* mutant

To generate a *bb0728 (cdr)* mutant, the entire *cdr* open-reading frame was first amplified by PCR from c162 using primers 2 and 3(Table 2) and TaKaRa *ExTaq* high fidelity polymerase (Fisher Scientific). The amplified fragment was digested with *Xho*I and *Bam*HI and ligated into digested pBSII-SK^+ (Stratagene), generating pBS-*cdr*. The *ermC* gene was amplified from pGK12 (Kok *et al*., 1984; Sartakova *et al*., 2000) (provided by F.C. Cabello, New York Medical College, Valhalla, New York) using primers 5 and 8 and cloned into pCR2.1-TOPO as instructed by the manufacturer (Invitrogen, Carlsbad, CA). The cloned *ermC* gene then was removed from its vector by digestion with *Eco* RI and ligated into *Eco* RI-digested pBS-*cdr*, which cuts within the *cdr* gene at positions 197 and 1203. The *cdr ::ermC* construct was amplified using the vector primers T7 and M13R.

Approximately 10 μg of amplified *cdr::ermC* was electroporated into electrocompetent c162, as previously described (Samuels, 1995; Eggers *et al*., 2002). Cells were electroporated and recovered at 33°C under either microaerobic or anaerobic conditions. After overnight recovery, each batch was expanded into 40 ml BSK-II supplemented with 0.06 μg/ml erythromycin and then dispensed into two 96-well plates in 200 μl aliquots, as described previously (Caimano *et al*., 2004). The samples were incubated under either standard or anaerobic conditions. Erythromycin-resistant spirochetes recovered under both conditions were then screened for the anticipated mutation by PCR using primers 1, 4, 6, and 7. Multiple clones with the correct mutation were recovered; one mutant, c309, was selected for further characterization. Plasmid content was determined by PCR as described previously (Eggers *et al*., 2002).

Transcriptional analysis of the cdr operon

Total RNA was isolated from c162 cultivated *in vitro* at 37°C to approximately 5×10^7 cells/ml in BSK-II under microaerobic conditions using TRIzol reagent according to the manufacturer's directions (Invitrogen). Contaminating DNA was removed using RQ1

RNase-free DNase (Promega) as previously described(Caimano *et al*., 2004). DNase-treated RNAs (1–4 μg total RNA per sample) were converted to cDNA using SuperScript First-Strand Synthesis for RT-PCR (Invitrogen) in the presence and absence of reverse transcriptase (RT) according to the manufacturer's instructions. The primers used to detect *bb0729* (10 & 12), *cdr* (13 & 15), and any transcript that extends between the two (11 & 14) are listed in Table 2. c162 DNA was used as a positive control and water alone was used as a negative control. Rapid amplification of the cDNA 5′-ends (5′-RACE) was performed using a 5′-RACE kit (Invitrogen) and the primers indicated in Table 2. Amplification using gene specific primers located within 5′ end of the *cdr* transcript yielded no product. The final product from the amplification of the region upstream of *bb0729* was cloned into pCR2.1-TOPO as instructed by the manufacturer (Invitrogen). The product was sequenced using the vector primers M13R and T7.

Complementation of the *cdr* mutation in c309

To complement c309, the entire *bb0729* and *cdr* open-reading frames, as well as a 500-bp segment upstream of *bb0729* were PCR-amplified using primers 4 and 9. The amplified product was cloned into pCR2.1-TOPO as instructed by the manufacturer. The fragment was digested from the vector with *Sac*I and *Not*I, purified from the gel using GeneClean II (Qbiogene), and ligated into *Sac*I-*Not*I digested pCE323 (Eggers *et al*., 2005). Ten μg of the resulting vector, pCE1735, were then transformed into c309 and selected on solid-phase plates supplemented with kanamycin (Samuels, 1995). Several kanamycin-resistant colonies were selected and analyzed to ensure that they contained pCE1735 and to determine their plasmid content (Eggers *et al*., 2002). One clone, c1655, was selected for further characterization.

Quantitative real time reverse transcriptase (RT)-PCR

Total RNA was isolated using TRIzol reagent (Invitrogen) as previously described(Mulay *et al*., 2009). Contaminating genomic DNA was removed using Turbo DNA*free* (Ambion, Inc. Austin, TX). DNase-treated RNAs (1–4 μg total RNA per sample) were converted to cDNA using SuperScript III (Invitrogen) in the presence and absence of reverse transcriptase (RT) according to the manufacturer's instructions. cDNAs (+RT) were assayed in quadruplicate using iQ Supermix (Bio-Rad). The primers used to detect *cdr* and *bb0729* transcripts are indicated in Table 2.*flaB* transcripts were assessed using SYBR Green or TaqMan probe-based assays. Transcript copy numbers were calculated using the iCycler post-run analysis software based on internal standard curves then normalized against copies of *flaB*.

Peroxide stress assays

For the oxidative stress assays, the densities of c162, c309, and c1655 were determined by darkfield microscopy using a Petroff-Hausser counting chamber. For each clone, 5 ml of BSK-II formulated without rabbit serum or BSA were inoculated to a density of 5×10^7 spirochetes per ml. Each tube was split into 4 × 1 ml aliquots and hydrogen peroxide or *t* -butyl hydroperoxide was added to the appropriate concentration (0–10 mM). The samples were incubated at 37°C for 1 h. After 1 h, 40 μl (2×10^6 cells) were added to 260 μl BSK-II and serially-diluted (1:1) to a final dilution of 2.4×10^{-1} spirochetes per well. Plates were placed at 37°C in a CO_2-incubator and monitored for growth over a 3 week period as indicated by a color change. Wells that did not exhibit a color change were analyzed for the presence of spirochetes by darkfield microscopy. Any well that had motile spirochetes at a density above background was considered positive. Each exposure assay was done in triplicate and the assay was performed four times. Alternatively, after exposure to varying concentrations of oxidizing agent, a dilution equivalent to 100 cells of each clone was plated in solid media with the appropriate antibiotic as previously described (Samuels, 1995; Boylan *et al*., 2008; Boylan and Gherardini, 2008). The number of viable cells recovered at

each concentration of oxidizing compound was compared to that recovered in the untreated samples. Each assay was performed in triplicate.

Growth curves

Growth kinetics of *B. burgdorferi* grown at 37°C *in vitro* under standard or anaerobic conditions were determined as follows. One hundred and fifty ml of media containing the appropriate antibiotic were inoculated with each isolate to a final density of 1×10^4 cells/ml and then distributed into ten 15 × 100 mm Petri dishes. One Petri dish each was placed in individual culture chambers under standard or anaerobic conditions. Multiple chambers were used to minimize the number of times cultures were exposed to atmospheric conditions. Starting with the third day after inoculation, one standard and one anaerobic chamber were opened and a sample of each culture removed for enumeration under darkfield using a Petroff-Hausser counting chamber (Hausser Scientific). Each *B. burgdorferi* clone was tested in triplicate. At intervals throughout the experiment, a 1 ml aliquot of culture was removed to confirm the consistency of the direct counts by using spectrophotometry as described previously (Samuels, 1995). For expression studies, RNA was harvested from samples in late exponential phase (Figure 6; arrows).

Mouse infectivity studies

To assess infectivity of wild-type and mutant *B. burgdorferi* strains, low-passage cultures were grown to mid-logarithmic density in BSK-II at 33°C. Five to eight week old C3H/HeJ or SCID (Jackson Laboratories) mice (five per group, per isolate) were inoculated intradermally with 10^4 spirochetes. Infection was determined four to eight weeks post-inoculation by cultivation of tissues in BSK-II medium and/or serologically, as indicated in results. For culturing, *Borrelia* antibiotic cocktail (0.05mg/ml sulphamethazole, 0.02 mg/ml phosphomycin, 0.05 mg/ml rifampicin, 0.01 mg/ml trimethoprin, and 0.0025 mg/ml amphotericin B) was added to the BSK-II to minimize contamination. In SCID mice, potential ankle swelling also was determined at four weeks post-inoculation. Serology was performed using whole cell lysates of wild-type *B. burgdorferi* grown at 37°C or purified recombinant OspC-HIS as previously described(Caimano *et al*., 2004; Mulay *et al*., 2009). All experimental procedures using mice were approved by and performed in accordance with the guidelines of the University of Connecticut Health Center Institutional Animal Care and Use Committee.

Tick-infection studies

To generate naturally-infected ticks, approximately 300–400 pathogen-free *I. scapularis* larvae (Oklahoma State University, Stillwater, OK) were placed on infected C3H/HeJ mice 2–3 weeks post-syringe inoculation, allowed to feed to repletion, then held in an environmental incubator until they had molted to the nymphal stage. To obtain fed nymphs, 10 to 12 infected unfed*Ixodes scapularis* nymphs were confined to a capsule affixed to the backs of naïve C3H/HeJ mice as previously described(Mulay *et al*., 2009). Immersion-fed larvae and nymphs were generated as previously described (Mulay *et al*., 2009) according to the method described by Policastro and Schwan (Policastro and Schwan, 2003). Rectal microinjection of naïve nymphs was performed as previously described (Pal *et al*., 2004).

Bioinformatics

To generate the sequence alignment given in Figure 1C, BLASTP using the *Bb* CoADR as a query was run against all microbial genomes in the NCBI database that corresponded (6/2011) to Gram-negative organisms and spirochetes, excluding *Borrelia*. Candidate CoADR orthologs were identified based on conservation of key active-site residues and CLUSTALX2 (Larkin *et al*., 2007) was used to generate an alignment of the 17 CoADR

sequences that resulted from distinct non-borrelial species. This alignment, which also includes *Sa* CoADR, *Ba* CoADR, *Ph* CoADR, and *Bb* CoADR, was then imported into ESPript (Gouet *et al*., 1999). Tthe SEED resource (Overbeek *et al*., 2005) was used for the identifaction of NAD(P)H-dependent dehydrogenases and reductases in *B. burgdorferi*..

Statistical analyses

To determine the statistical significance of observed differences, matching data points ($n \geq 3$) were compared within GraphPad Prism v4.00 (GraphPad Software, San Diego, CA,USA) using an unpaired *t* -test with two-tailed *P* -values and a 95% confidence interval. Asterisks indicate a level of significance where $P < 0.05$. Error bars represent the standard error of the mean (SEM).

Acknowledgments

We gratefully acknowledge the expert technical assistance of Morgan LeDoyt, Anna Allard, and Cynthia Gonzalez. We also thank Drs. Frank Gherardini (Rocky Mountain Laboratories), Julie Boylan (Rocky Mountain Laboratories), Star Dunham-Ems (University of Connecticut Health Center), Amit Luthra (University of Connecticut Health Center), and Arvind Anan (University of Connecticut Health Center) for valuable discussions and/or for sharing unpublished data.

Funding for this work was provided by AI-29735 (JDR and MJC), 3R01AI029735-20S1 (JDR and MJC), AI-26756 (JDR), AI085248 (MJC), AI-10573 (KROH), AI-080615 (UP), North Carolina Biotechnology Center grant 2011-MRG-1116 (AC),and the National Research Fund for Tick-Borne Diseases (MJC). Additional funding was provided by a Quinnipiac University School of Health Sciences Faculty Research Award (C.H.E.) and a QU Summer Undergraduate Research Fellowship (R.M.).

References

Anguita J, Hedrick MN, Fikrig E. Adaptation of *Borrelia burgdorferi* in the tick and the mammalian host. FEMS Microbiol Rev. 2003; 27:493–504. [PubMed: 14550942]

Argyrou A, Blanchard JS. Flavoprotein disulfide reductases: advances in chemistry and function. Prog Nucleic Acid Res Mol Biol. 2004; 78:89–142. [PubMed: 15210329]

Arnold K, Bordoli L, Kopp J, Schwede T. The SWISS-MODEL workspace: a web-based environment for protein structure homology modelling. Bioinformatics. 2006; 22:195–201. [PubMed: 16301204]

Ausubel, FM.; Brent, R.; Kingston, RE.; Moore, DD.; Seidman, JG.; Smith, JA.; Struhl, K. Short Protocols in Molecular Biology. New York: John Wiley & Sons; 1997.

Benhnia MR, Wroblewski D, Akhtar MN, Patel RA, Lavezzi W, Gangloff SC, et al. Signaling through CD14 attenuates the inflammatory response to *Borrelia burgdorferi*, the agent of Lyme disease. J Immunol. 2005; 174:1539–1548. [PubMed: 15661914]

Blevins JS, Xu H, He M, Norgard MV, Reitzer L, Yang XF. Rrp2, a sigma54-dependent transcriptional activator of *Borrelia burgdorferi*, activates *rpoS* in an enhancer-independent manner. J Bacteriol. 2009; 191:2902–2905. [PubMed: 19201806]

Boardman BK, He M, Ouyang Z, Xu H, Pang X, Yang XF. Essential role of the response regulator Rrp2 in the infectious cycle of Borrelia burgdorferi. Infect Immun. 2008; 76:3844–3853. [PubMed: 18573895]

Bordoli L, Kiefer F, Arnold K, Benkert P, Battey J, Schwede T. Protein structure homology modeling using SWISS-MODEL workspace. Nat Protoc. 2009; 4:1–13. [PubMed: 19131951]

Boylan JA, Gherardini FC. Determining the cellular targets of reactive oxygen species in Borrelia burgdorferi. Methods Mol Biol. 2008; 431:213–221. [PubMed: 18287759]

Boylan JA, Hummel CS, Benoit S, Garcia-Lara J, Treglown-Downey J, Crane EJ III, Gherardini FC. Borrelia burgdorferibb0728 encodes a coenzyme A disulphide reductase whose function suggests a role in intracellular redox and the oxidative stress response. Mol Microbiol. 2006; 59:475–486. [PubMed: 16390443]

Boylan JA, Lawrence KA, Downey JS, Gherardini FC. Borrelia burgdorferi membranes are the primary targets of reactive oxygen species. Mol Microbiol. 2008; 68:786–799. [PubMed: 18373524]

Boylan JA, Posey JE, Gherardini FC. Borrelia oxidative stress response regulator, BosR: a distinctive Zn-dependent transcriptional activator. Proc Natl Acad Sci U S A. 2003; 100:11684–11689. [PubMed: 12975527]

Burguiere P, Auger S, Hullo MF, Danchin A, Martin-Verstraete I. Three different systems participate in L-cystine uptake in Bacillus subtilis. J Bacteriol. 2004; 186:4875–4884. [PubMed: 15262924]

Cabiscol E, Tamarit J, Ros J. Oxidative stress in bacteria and protein damage by reactive oxygen species. Int Microbiol. 2000; 3:3–8. [PubMed: 10963327]

Caimano MJ, Eggers CH, Gonzalez C, Radolf JD. Alternate sigma factor, RpoS, is required for the *in vivo* -specific repression of the *Borrelia burgdorferi* lp54-borne *ospA* and *lp6.6* genes. J Bacteriol. 2005; 187:7845–7852. [PubMed: 16267308]

Caimano MJ, Eggers CH, Hazlett KR, Radolf JD. RpoS is not central to the general stress response in *Borrelia burgdorferi*, but does control expression of one or more essential virulence determinants. Infect Immun. 2004; 72:6433–6445. [PubMed: 15501774]

Caimano MJ, Iyer R, Eggers CH, Gonzalez C, Morton EA, Gilbert MA, et al. Analysis of the RpoS regulon in *Borrelia burgdorferi* in response to mammalian host signals provides insight into RpoS function during the enzootic cycle. Mol Microbiol. 2007; 65:1193–1217. [PubMed: 17645733]

Carmel-Harel O, Storz G. Roles of the glutathione- and thioredoxin-dependent reduction systems in the *Escherichia coli* and *Saccharomyces cerevisiae* responses to oxidative stress. Annu Rev Microbiol. 2000a; 54:439–461. [PubMed: 11018134]

Carmel-Harel O, Storz G. Roles of the glutathione- and thioredoxin-dependent reduction systems in the Escherichia coli and saccharomyces cerevisiae responses to oxidative stress. Annu Rev Microbiol. 2000b; 54:439–461. [PubMed: 11018134]

Chan DI, Vogel HJ. Current understanding of fatty acid biosynthesis and the acyl carrier protein. Biochem J. 2010; 430:1–19. [PubMed: 20662770]

delCardayre SB, Davies JE. Staphylococcus aureus coenzyme A disulfide reductase, a new subfamily of pyridine nucleotide-disulfide oxidoreductase. Sequence, expression, and analysis of cdr. J Biol Chem. 1998; 273:5752–5757. [PubMed: 9488708]

delCardayre SB, Stock KP, Newton GL, Fahey RC, Davies JE. Coenzyme A disulfide reductase, the primary low molecular weight disulfide reductase from *Staphylococcus aureus*. Purification and characterization of the native enzyme. J Biol Chem. 1998; 273:5744–5751. [PubMed: 9488707]

Dolan MC, Piesman J, Schneider BS, Schriefer M, Brandt K, Zeidner NS. Comparison of disseminated and nondisseminated strains of *Borrelia burgdorferi* sensu stricto in mice naturally infected by tick bite. Infect Immun. 2004; 72:5262–5266. [PubMed: 15322021]

Dunham-Ems SM, Caimano MJ, Pal U, Wolgemuth CW, Eggers CH, Balic A, Radolf JD. Live imaging reveals a biphasic mode of dissemination of *Borrelia burgdorferi* within ticks. J Clin Invest. 2009; 119:3652–3665. [PubMed: 19920352]

Eggers CH, Caimano MJ, Clawson ML, Miller WG, Samuels DS, Radolf JD. Identification of loci critical for replication and compatibility of a *Borrelia burgdorferi* cp32 plasmid and use of a cp32-based shuttle vector for the expression of fluorescent reporters in the Lyme disease spirochaete. Mol Microbiol. 2002; 43:281–295. [PubMed: 11985709]

Eggers CH, Caimano MJ, Radolf JD. Analysis of promoter elements involved in the transcriptional initiation of RpoS-dependent *Borrelia burgdorferi* genes. J Bacteriol. 2004; 186:7390–7402. [PubMed: 15489451]

Eggers CH, Caimano MJ, Radolf JD. Sigma factor selectivity in *Borrelia burgdorferi* : RpoS recognition of the *ospE* /*ospF* /*elp* promoters is dependent upon the sequence of the −10 region. Mol Microbiol. 2005; 59:1859–1875. [PubMed: 16553889]

Esteve-Gassent MD, Elliott NL, Seshu J. sodA is essential for virulence of *Borrelia burgdorferi* in the murine model of Lyme disease. Mol Microbiol. 2009; 71:594–612. [PubMed: 19040638]

Fisher MA, Grimm D, Henion AK, Elias AF, Stewart PE, Rosa PA, Gherardini FC. Borrelia burgdorferi σ^{54} is required for mammalian infection and vector transmission but not for tick colonization. Proc Natl Acad Sci U S A. 2005; 102:5162–5167. [PubMed: 15743918]

Fraser CM, Casjens S, Huang WM, Sutton GG, Clayton R, Lathigra R, et al. Genomic sequence of a Lyme disease spirochaete, Borrelia burgdorferi. Nature. 1997; 390:580–586. [PubMed: 9403685]

Gaballa A, Newton GL, Antelmann H, Parsonage D, Upton H, Rawat M, et al. Biosynthesis and functions of bacillithiol, a major low-molecular-weight thiol in Bacilli. Proc Natl Acad Sci U S A. 2010; 107:6482–6486. [PubMed: 20308541]

Ge Y, Old IG, Girons IS, Charon NW. The *flgK* motility operon of *Borrelia burgdorferi* is initiated by a σ^{70}-like promoter. Microbiology. 1997; 143 (Pt 5):1681–1690. [PubMed: 9168617]

Gherardini, FC.; Boylan, JA.; Lawrence, K.; Skare, JT. Metabolism and Physiology of Borrelia. In: Samuels, DS.; Radolf, JD., editors. *Borrelia*: Molecular Biology, Host Interaction and Pathogenesis. Norfolk UK: Caister Academic Press; 2010. p. 139-166.

Gibson CM, Mallett TC, Claiborne A, Caparon MG. Contribution of NADH oxidase to aerobic metabolism of Streptococcus pyogenes. J Bacteriol. 2000; 182:448–455. [PubMed: 10629192]

Gouet P, Courcelle E, Stuart DI, Metoz F. ESPript: analysis of multiple sequence alignments in PostScript. Bioinformatics. 1999; 15:305–308. [PubMed: 10320398]

Harris DR, Ward DE, Feasel JM, Lancaster KM, Murphy RD, Mallet TC, Crane EJ III. Discovery and characterization of a Coenzyme A disulfide reductase from *Pyrococcus horikoshii*. Implications for this disulfide metabolism of anaerobic hyperthermophiles. FEBS J. 2005; 272:1189–1200. [PubMed: 15720393]

Higuchi M, Yamamoto Y, Poole LB, Shimada M, Sato Y, Takahashi N, Kamio Y. Functions of two types of NADH oxidases in energy metabolism and oxidative stress of Streptococcus mutans. J Bacteriol. 1999; 181:5940–5947. [PubMed: 10498705]

Hodzic E, Feng S, Freet KJ, Barthold SW. Borrelia burgdorferi population dynamics and prototype gene expression during infection of immunocompetent and immunodeficient mice. Infect Immun. 2003; 71:5042–5055. [PubMed: 12933847]

Holmgren A. Thioredoxin and glutaredoxin systems. J Biol Chem. 1989; 264:13963–13966. [PubMed: 2668278]

Holmgren A. Antioxidant function of thioredoxin and glutaredoxin systems. Antioxid Redox Signal. 2000; 2:811–820. [PubMed: 11213485]

Holmgren A, Johansson C, Berndt C, Lonn ME, Hudemann C, Lillig CH. Thiol redox control via thioredoxin and glutaredoxin systems. Biochem Soc Trans. 2005; 33:1375–1377. [PubMed: 16246122]

Hubner A, Yang X, Nolen DM, Popova TG, Cabello FC, Norgard MV. Expression of *Borrelia burgdorferi* OspC and DbpA is controlled by a RpoN-RpoS regulatory pathway. Proc Natl Acad Sci U S A. 2001; 98:12724–12729. [PubMed: 11675503]

Hummel CS, Lancaster KM, Crane EJ III. Determination of coenzyme A levels in *Pyrococcus furiosus* and other Archaea: implications for a general role for coenzyme A in thermophiles. FEMS Microbiol Lett. 2005; 252:229–234. [PubMed: 16213671]

Hyde JA, Shaw DK, Smith IR, Trzeciakowski JP, Skare JT. The BosR regulatory protein of *Borrelia burgdorferi* interfaces with the RpoS regulatory pathway and modulates both the oxidative stress response and pathogenic properties of the Lyme disease spirochete. Mol Microbiol. 2009; 74:1344–1355. [PubMed: 19906179]

Imlay JA. How oxygen damages microbes: oxygen tolerance and obligate anaerobiosis. Adv Microb Physiol. 2002; 46:111–153. [PubMed: 12073652]

Imlay JA. Pathways of oxidative damage. Annu Rev Microbiol. 2003; 57:395–418. [PubMed: 14527285]

Imlay JA. Cellular defenses against superoxide and hydrogen peroxide. Annu Rev Biochem. 2008; 77:755–776. [PubMed: 18173371]

Jackowski, S. Biosynthesis of Pantothenic Acid and Coenzyme A. In: Neidhardt, FC.; Curtiss, R.; Gross, CA.; Ingraham, JL.; Lin, ECC.; Low, KB., editors. *Esherichia coli* and *Salmonella typhimurium* : cellular and molecular biology. Washington D.C: American Society for Microbiology; 1996. p. 687-694.

Jackowski S, Rock CO. Regulation of coenzyme A biosynthesis. J Bacteriol. 1981; 148:926–932. [PubMed: 6796563]

Kadokura H, Katzen F, Beckwith J. Protein disulfide bond formation in prokaryotes. Annu Rev Biochem. 2003; 72:111–135. [PubMed: 12524212]

Kariu T, Coleman AS, Anderson JF, Pal U. Methods for rapid transfer and localization of lyme disease pathogens within the tick gut. J Vis Exp. 2011

Karna SL, Sanjuan E, Esteve-Gassent MD, Miller CL, Maruskova M, Seshu J. CsrA modulates levels of lipoproteins and key regulators of gene expression critical for pathogenic mechanisms of Borrelia burgdorferi. Infect Immun. 2011; 79:732–744. [PubMed: 21078860]

Karplus PA, Schulz GE. Substrate binding and catalysis by glutathione reductase as derived from refined enzyme: substrate crystal structures at 2 A resolution. J Mol Biol. 1989; 210:163–180. [PubMed: 2585516]

Katona LI, Tokarz R, Kuhlow CJ, Benach J, Benach JL. The fur homologue in Borrelia burgdorferi. J Bacteriol. 2004; 186:6443–6456. [PubMed: 15375125]

Kok J, van dV, Venema . Construction of plasmid cloning vectors for lactic streptococci which also replicate in *Bacillus subtilis* and Escherichia coli. Appl Environ Microbiol. 1984; 48:726–731. [PubMed: 6095756]

Labandeira-Rey M, Seshu J, Skare JT. The absence of linear plasmid 25 or 28-1 of *Borrelia burgdorferi* dramatically alters the kinetics of experimental infection via distinct mechanisms. Infect Immun. 2003; 71:4608–4613. [PubMed: 12874340]

Labandeira-Rey M, Skare JT. Decreased infectivity in *Borrelia burgdorferi* strain B31 is associated with loss of linear plasmid 25 or 28-1. Infect Immun. 2001; 69:446–455. [PubMed: 11119536]

Lane RS, Piesman J, Burgdorfer W. Lyme borreliosis: relation of its causative agent to its vectors and hosts in North America and Europe. Annu Rev Entomol. 1991; 36:587–609. [PubMed: 2006870]

Larkin MA, Blackshields G, Brown NP, Chenna R, McGettigan PA, McWilliam H, et al. Clustal W and Clustal X version 2.0. Bioinformatics. 2007; 23:2947–2948. [PubMed: 17846036]

Lawrenz MB, Wooten RM, Norris SJ. Effects of vlsE complementation on the infectivity of *Borrelia burgdorferi* lacking the linear plasmid lp28-1. Infect Immun. 2004; 72:6577–6585. [PubMed: 15501789]

Li X, Pal U, Ramamoorthi N, Liu X, Desrosiers DC, Eggers CH, et al. The Lyme disease agent *Borrelia burgdorferi* requires BB0690, a Dps homologue, to persist within ticks. Mol Microbiol. 2007; 63:694–710. [PubMed: 17181780]

Mallett TC, Wallen JR, Karplus PA, Sakai H, Tsukihara T, Claiborne A. Structure of coenzyme A-disulfide reductase from *Staphylococcus aureus* at 1.54 A resolution. Biochemistry. 2006; 45:11278–11289. [PubMed: 16981688]

McDowell JV, Sung SY, Hu LT, Marconi RT. Evidence that the variable regions of the central domain of VlsE are antigenic during infection with lyme disease spirochetes. Infect Immun. 2002; 70:4196–4203. [PubMed: 12117928]

Mulay VB, Caimano MJ, Iyer R, Dunham-Ems S, Liveris D, Petzke MM, et al. Borrelia burgdorferi bba74 is expressed exclusively during tick feeding and is regulated by both arthropod- and mammalian host-specific signals. J Bacteriol. 2009; 191:2783–2794. [PubMed: 19218390]

Newton GL, Arnold K, Price MS, Sherrill C, delCardayre SB, Aharonowitz Y, et al. Distribution of thiols in microorganisms: mycothiol is a major thiol in most actinomycetes. J Bacteriol. 1996; 178:1990–1995. [PubMed: 8606174]

Newton GL, Buchmeier N, Fahey RC. Biosynthesis and functions of mycothiol, the unique protective thiol of Actinobacteria. Microbiol Mol Biol Rev. 2008; 72:471–494. [PubMed: 18772286]

Newton GL, Rawat M, La Clair JJ, Jothivasan VK, Budiarto T, Hamilton CJ, et al. Bacillithiol is an antioxidant thiol produced in Bacilli. Nat Chem Biol. 2009; 5:625–627. [PubMed: 19578333]

Nicely NI, Parsonage D, Paige C, Newton GL, Fahey RC, Leonardi R, et al. Structure of the type III pantothenate kinase from *Bacillus anthracis* at 2.0 A resolution: implications for coenzyme A-dependent redox biology. Biochemistry. 2007; 46:3234–3245. [PubMed: 17323930]

Ojha S, Meng EC, Babbitt PC. Evolution of function in the “two dinucleotide binding domains” flavoproteins. PLoS Comput Biol. 2007; 3:e121. [PubMed: 17658942]

Ouyang Z, Blevins JS, Norgard MV. Transcriptional interplay among the regulators Rrp2, RpoN and RpoS in Borrelia burgdorferi. Microbiology. 2008; 154:2641–2658. [PubMed: 18757798]

Ouyang Z, Deka RK, Norgard MV. BosR (BB0647) Controls the RpoN-RpoS Regulatory Pathway and Virulence Expression in *Borrelia burgdorferi* by a Novel DNA-Binding Mechanism. PLoS Pathog. 2011; 7:e1001272. [PubMed: 21347346]

Ouyang Z, Kumar M, Kariu T, Haq S, Goldberg M, Pal U, Norgard MV. BosR (BB0647) governs virulence expression in Borrelia burgdorferi. Mol Microbiol. 2009; 74:1331–1343. [PubMed: 19889086]

Overbeek R, Begley T, Butler RM, Choudhuri JV, Chuang HY, Cohoon M, et al. The subsystems approach to genome annotation and its use in the project to annotate 1000 genomes. Nucleic Acids Res. 2005; 33:5691–5702. [PubMed: 16214803]

Paige C, Reid SD, Hanna PC, Claiborne A. The type III pantothenate kinase encoded by coaX is essential for growth of Bacillus anthracis. J Bacteriol. 2008; 190:6271–6275. [PubMed: 18641144]

Pal U, Fikrig E. Adaptation of *Borrelia burgdorferi* in the vector and vertebrate host. Microbes and Infection. 2003; 5:659–666. [PubMed: 12787742]

Pal U, Yang X, Chen M, Bockenstedt LK, Anderson JF, Flavell RA, et al. OspC facilitates *Borrelia burgdorferi* invasion of Ixodes scapularis salivary glands. J Clin Invest. 2004; 113:220–230. [PubMed: 14722614]

Parsonage D, Desrosiers DC, Hazlett KR, Sun Y, Nelson KJ, Cox DL, et al. Broad specificity AhpC-like peroxiredoxin and its thioredoxin reductant in the sparse antioxidant defense system of Treponema pallidum. Proc Natl Acad Sci U S A. 2010; 107:6240–6245. [PubMed: 20304799]

Parsonage D, Karplus PA, Poole LB. Substrate specificity and redox potential of AhpC, a bacterial peroxiredoxin. Proc Natl Acad Sci U S A. 2008; 105:8209–8214. [PubMed: 18165315]

Piesman J, Schneider BS, Zeidner NS. Use of quantitative PCR to measure density of *Borrelia burgdorferi* in the midgut and salivary glands of feeding tick vectors. J Clin Microbiol. 2001; 39:4145–4148. [PubMed: 11682544]

Piesman J, Zeidner NS, Schneider BS. Dynamic changes in *Borrelia burgdorferi* populations in Ixodes scapularis (Acari: Ixodidae) during transmission: studies at the mRNA level. Vector Borne Zoonotic Dis. 2003; 3:125–132. [PubMed: 14511582]

Policastro PF, Schwan TG. Experimental infection of *Ixodes scapularis* larvae (Acari: Ixodidae) by immersion in low passage cultures of Borrelia burgdorferi. J Med Entomol. 2003; 40:364–370. [PubMed: 12943118]

Poole LB. Bacterial defenses against oxidants: mechanistic features of cysteine-based peroxidases and their flavoprotein reductases. Arch Biochem Biophys. 2005; 433:240–254. [PubMed: 15581580]

Samuels DS. Electrotransformation of the spirochete *Borrelia burgdorferi*. Electrotransformation protocols for microorgansims. Method Mol Biol. 1995; 47:253–259.

Sanjuan E, Esteve-Gassent MD, Maruskova M, Seshu J. Overexpression of CsrA (BB0184) alters the morphology and antigen profiles of Borrelia burgdorferi. Infect Immun. 2009; 77:5149–5162. [PubMed: 19737901]

Sartakova M, Dobrikova E, Cabello FC. Development of an extrachromosomal cloning vector system for use in Borrelia burgdorferi. Proc Natl Acad Sci U S A. 2000; 97:4850–4855. [PubMed: 10781091]

Seshu J, Boylan JA, Gherardini FC, Skare JT. Dissolved oxygen levels alter gene expression and antigen profiles in Borrelia burgdorferi. Infect Immun. 2004; 72:1580–1586. [PubMed: 14977964]

Seshu J, Skare JT. The many faces of Borrelia burgdorferi. J Mol Microbiol Biotechnol. 2000; 2:463–472. [PubMed: 11075919]

Sevier CS, Kaiser CA. Formation and transfer of disulphide bonds in living cells. Nat Rev Mol Cell Biol. 2002; 3:836–847. [PubMed: 12415301]

Sorci G, Faivre B. Inflammation and oxidative stress in vertebrate host-parasite systems. Philos Trans R Soc Lond B Biol Sci. 2009; 364:71–83. [PubMed: 18930878]

Stanton TB, Rosey EL, Kennedy MJ, Jensen NS, Bosworth BT. Isolation, oxygen sensitivity, and virulence of NADH oxidase mutants of the anaerobic spirochete *Brachyspira* (*Serpulina*) *hyodysenteriae*, etiologic agent of swine dysentery. Appl Environ Microbiol. 1999; 65:5028–5034. [PubMed: 10543819]

Steere AC, Coburn J, Glickstein L. The emergence of Lyme disease. J Clin Invest. 2004; 113:1093–1101. [PubMed: 15085185]

Steere AC, Grodzicki RL, Craft JE, Shrestha M, Kornblatt AN, Malawista SE. Recovery of Lyme disease spirochetes from patients. Yale J Biol Med. 1984; 57:557–560. [PubMed: 6393606]

Stehle T, Claiborne A, Schulz GE. NADH binding site and catalysis of NADH peroxidase. Eur J Biochem. 1993; 211:221–226. [PubMed: 8425532]

Sze CW, Li C. Inactivation of bb0184, Which Encodes Carbon Storage Regulator A, Represses the Infectivity of Borrelia burgdorferi. Infect Immun. 2011; 79:1270–1279. [PubMed: 21173314]

Tilly K, Elias AF, Errett J, Fischer E, Iyer R, Schwartz I, et al. Genetics and regulation of chitobiose utilization in Borrelia burgdorferi. J Bacteriol. 2001; 183:5544–5553. [PubMed: 11544216]

Tilly K, Rosa PA, Stewart PE. Biology of infection with Borrelia burgdorferi. Infect Dis Clin North Am. 2008; 22:217–234. [PubMed: 18452798]

Wallen JR, Mallett TC, Boles W, Parsonage D, Furdui CM, Karplus PA, Claiborne A. Crystal structure and catalytic properties of *Bacillus anthracis* CoADR-RHD: implications for flavin-linked sulfur trafficking. Biochemistry. 2009; 48:9650–9667. [PubMed: 19725515]

Wallen JR, Paige C, Mallett TC, Karplus PA, Claiborne A. Pyridine nucleotide complexes with *Bacillus anthracis* coenzyme A-disulfide reductase: a structural analysis of dual NAD(P)H specificity. Biochemistry. 2008; 47:5182–5193. [PubMed: 18399646]

Wolfe AJ. The acetate switch. Microbiol Mol Biol Rev. 2005; 69:12–50. [PubMed: 15755952]

Xu H, Caimano MJ, Lin T, He M, Radolf JD, Norris SJ, et al. Role of acetyl-phosphate in activation of the Rrp2-RpoN-RpoS pathway in Borrelia burgdorferi. PLoS Pathog. 2010; 6

Yang XF, Alani SM, Norgard MV. The response regulator Rrp2 is essential for the expression of major membrane lipoproteins in Borrelia burgdorferi. Proc Natl Acad Sci U S A. 2003; 100:11001–11006. [PubMed: 12949258]

Ying W. NAD+ and NADH in cellular functions and cell death. Front Biosci. 2006; 11:3129–3148. [PubMed: 16720381]

Ying W. NAD+/NADH and NADP+/NADPH in cellular functions and cell death: regulation and biological consequences. Antioxid Redox Signal. 2008; 10:179–206. [PubMed: 18020963]

Zeidner NS, Schneider BS, Dolan MC, Piesman J. An analysis of spirochete load, strain, and pathology in a model of tick-transmitted Lyme borreliosis. Vector Borne Zoonotic Dis. 2001; 1:35–44. [PubMed: 12653134]

Zhang X, Yang X, Kumar M, Pal U. BB0323 function is essential for *Borrelia burgdorferi* virulence and persistence through tick-rodent transmission cycle. J Infect Dis. 2009; 200:1318–1330. [PubMed: 19754308]

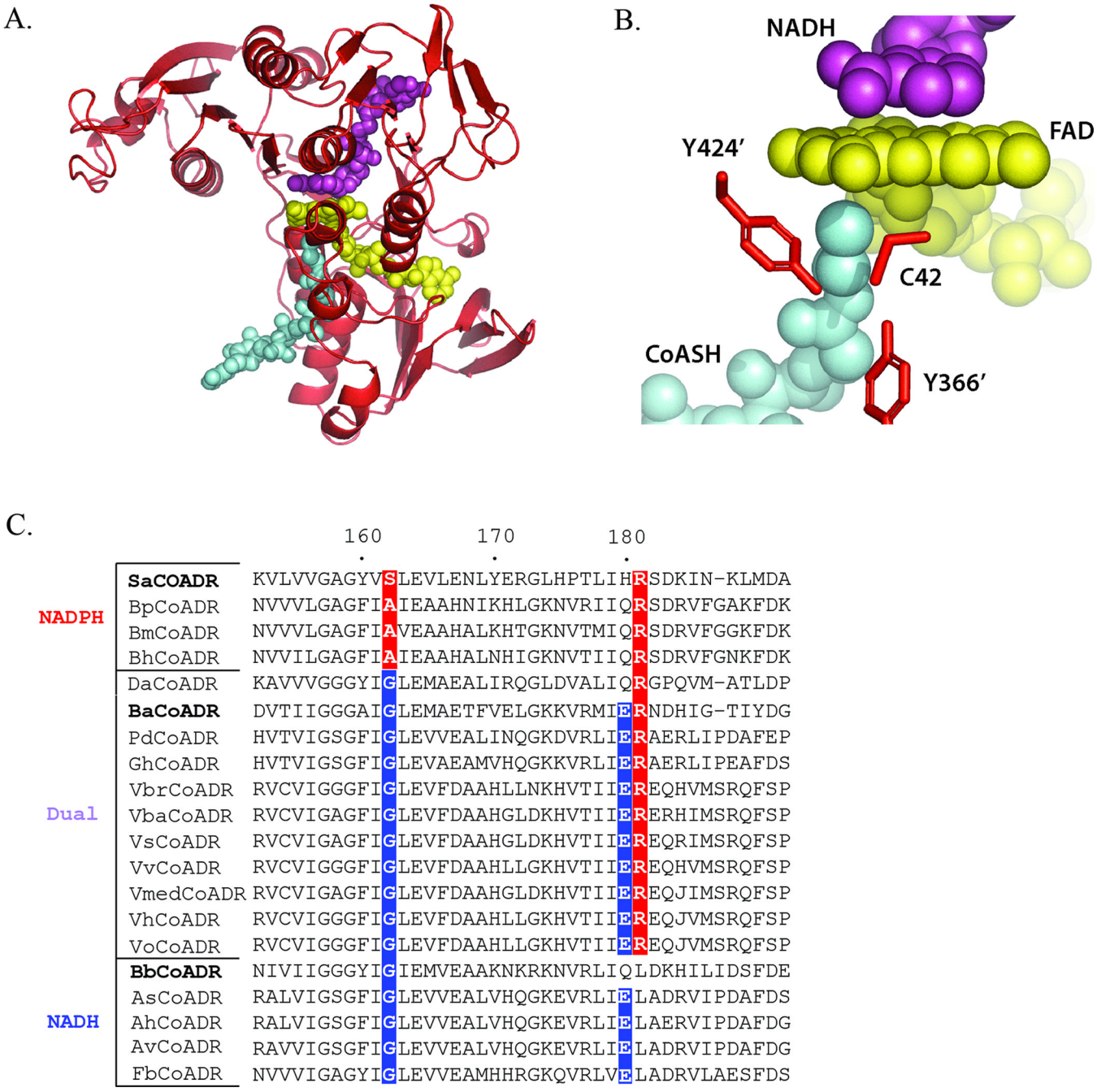

Figure 1.

(A) A monomer of a *Bb* CoADR homology model generated based on the structure of the reduced *Ba* CoADR-NADH complex (Wallen *et al*., 2008). CoASH, FAD, and NADH are colored cyan, yellow, and magenta, respectively. The orientation is the same as Figure 3 published in (Wallen*et al*., 2008). PDB code for the *Ba* CoADR structure used is 3CGD. (B) The predicted active site of *Bb* CoADR. *Bb* CoADR residues [Cys 42 (chain A) and Tyr366' and Tyr424' (chain B)] are indicated. CoASH, FAD, and NADH are colored the same as in (B).(C) Sequence alignment for the NAD(P)H-binding motifs of annotated CoADRs from Gram negative bacteria and spirochetes. Sequence numbering corresponds to *Ba* CoADR. Gly at position 162 and Asp or Glu at position 180 are favored for NADH-specificity, while

Ala and Arg residues at positions 162 and 181, respectively, contribute to NADPH-specificity (Karplus and Schulz, 1989; Stehle *et al*., 1993; Wallen *et al*., 2008). A hybrid sequence of Glu180 and Arg181 is characteristic of dual NADH and NADPH specificity (Wallen *et al*., 2008). Enzymes are grouped according to predicted NAD(P)H substrate preference; positions important for NADPH- (red) or NADH- (blue) specificity are indicated. CoADRs with experimentally-determined pyridine nucleotide specificity are indicated in bold. Bp, *Br. pilisicoli* ; Bm, *Br. murdochii* ; Bh, *Br. hyodysenteriae* ; Da, *D. acetoxidans* ; Pd, *Photobacterium damselae* ; Gh, *Grimontia hollisae* ; Vbr, *Vibrio brasiliensis* ; Vba, *V. bacterium* ; Vs, *V. splendidus* ; Vv, *V. vulnificus* ; Vmed, *V. sp.* MED22; Vh, *V. harveyi* ; Vo, *V. orientalis* ; As, *A. salmonicidia* ; Ah, *A. hydrophila* ; Av, *A. veronii* ; Fb, *F. balearica*.

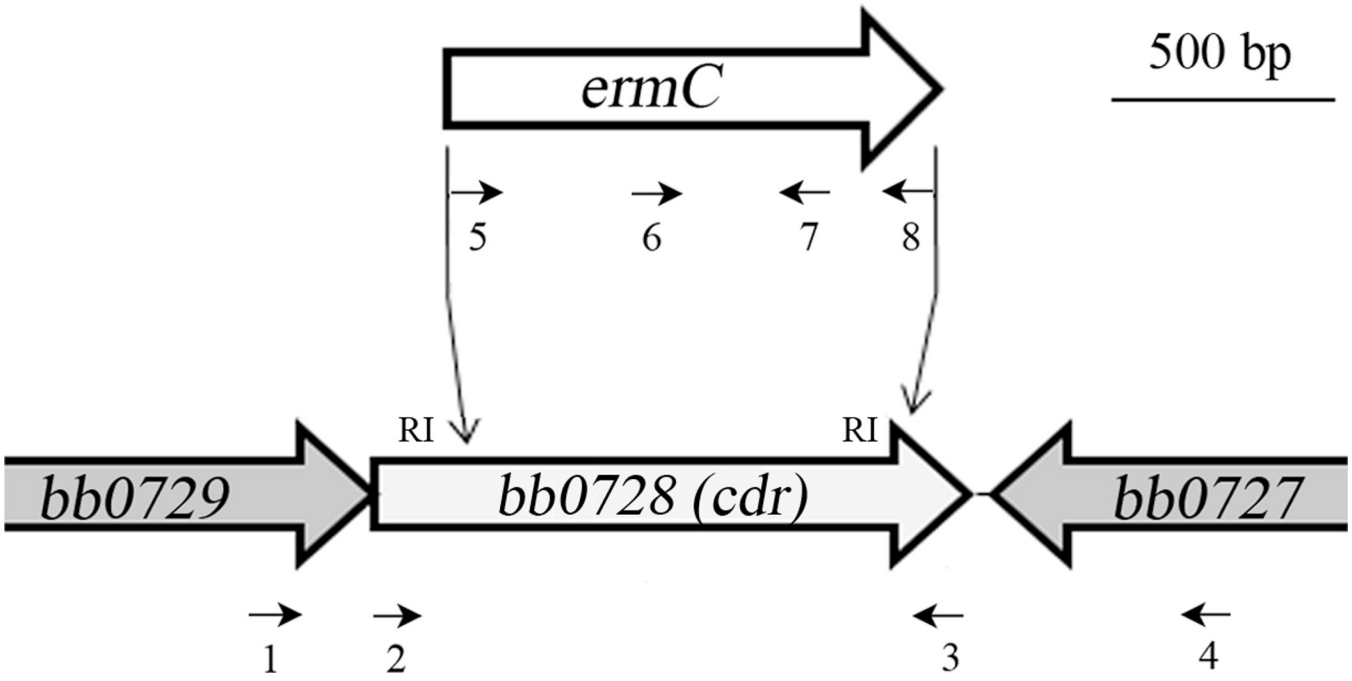

Figure 2.

Generation of a *cdr* -mutant in a virulent clone of *B. burgdorferi* strain 297. An erythromycin-resistance cassette (*ermC*) was cloned into two endogenous *Eco*RI (RI) sites within *bb0728 (cdr)* in c162. Oligonucleotoide primers used for the generation and screening of the mutant are indicated by small arrows. Numbers correspond to primers found in Table 2.

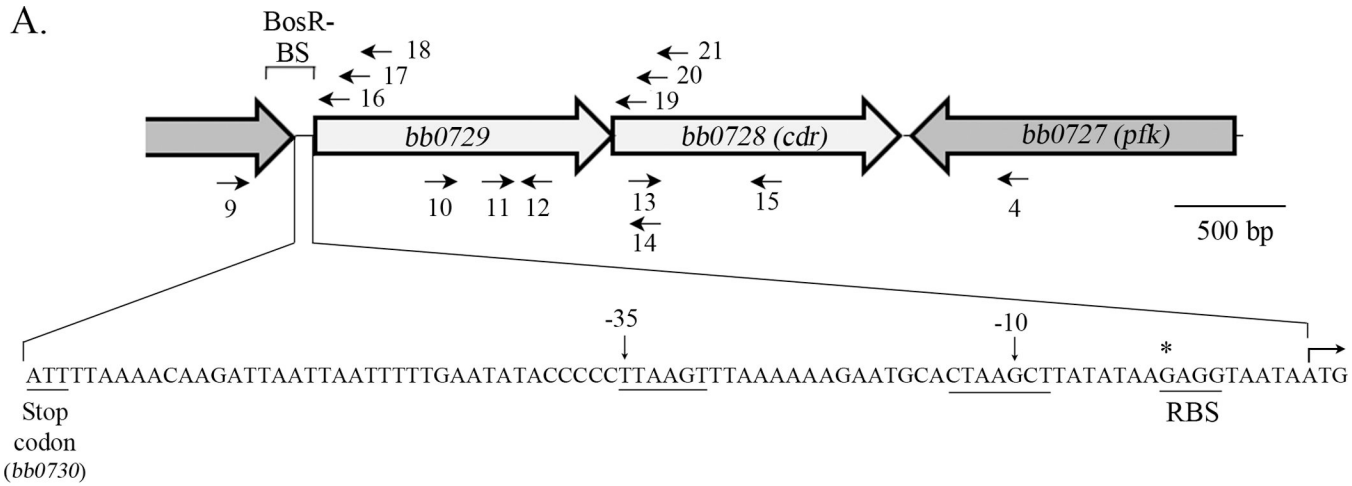

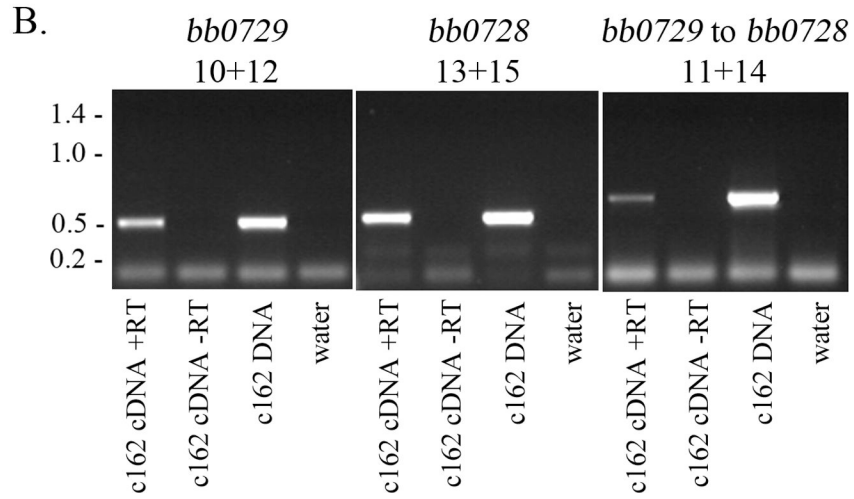

Figure 3.

The *bb0729 cdr* operon. (A) Organization of the region surrounding *bb0728 (cdr)*. Primers used to demonstrate the presence of a single transcript are indicated below the gene diagram; primers used for 5′-RACE to determine promoter location(s) are shown above the gene diagram. The region in which BosR potentially binds (Boylan *et al*., 2006) is indicated (BosR-BS). The transcriptional start site (*), ribosomal binding site (RBS) and −10/−35 elements, as determined by 5′-RACE, are shown within the region between *bb0730* and *bb0729*. (B) *bb0729* and the *cdr* gene are co-transcribed under the regulatory control of a promoter upstream of *bb0729*. C162 was grown to 5×10^7 cells/ml at 37°C under standard conditions. RNA was harvested, converted to cDNA, and analyzed by RT-PCR using the indicated primer pairs; the corresponding locations for the primers (Table 2) are shown in (A). Molecular weights are given in kbp.

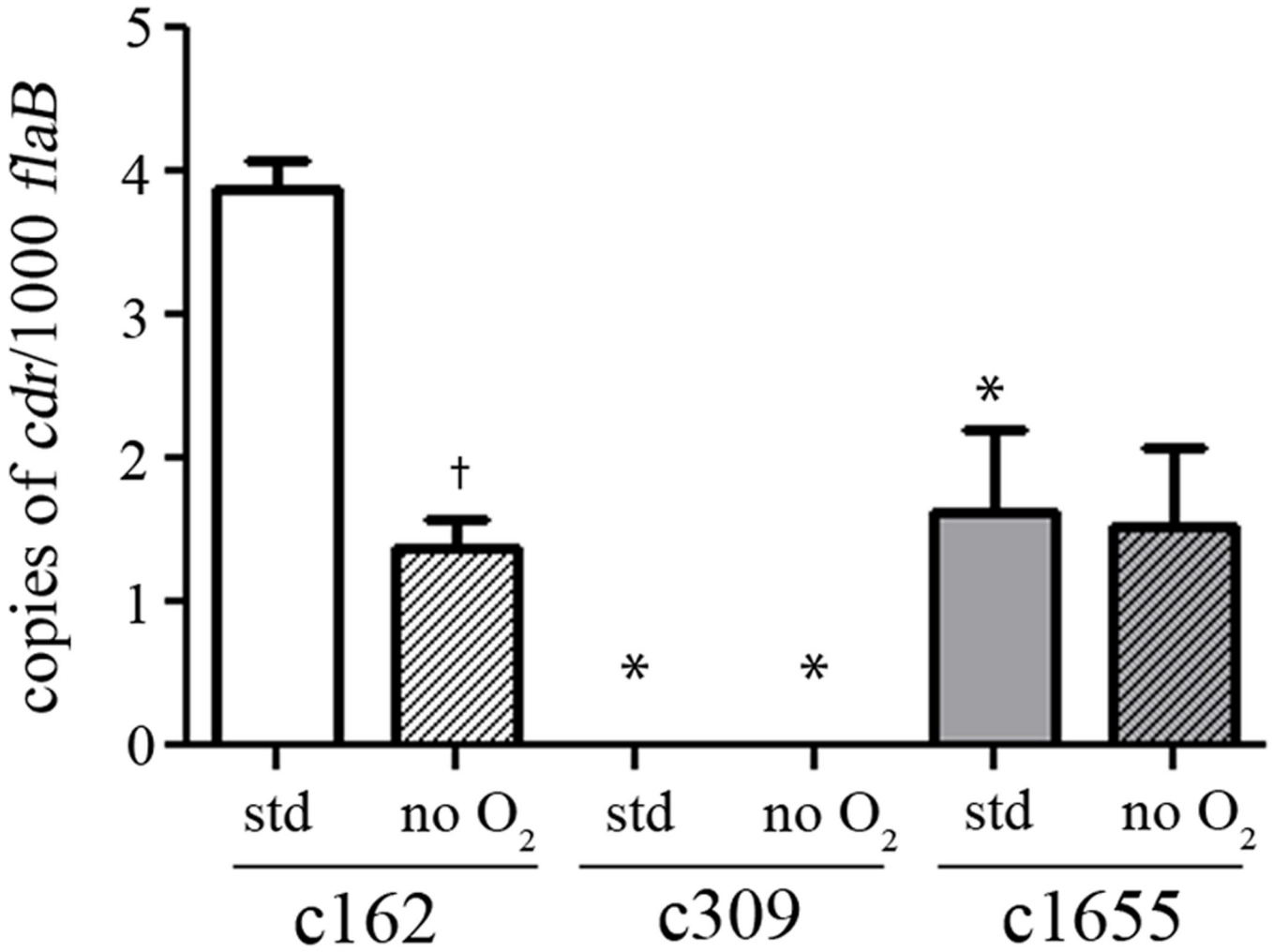

Figure 4.

Transcriptional analyses of *cdr* expression in c162 (wt), c309 (mut), and c1655 (ct) grown *in vitro* under standard and anaerobic conditions. RNAs were harvested from spirochetes grown to late exponential phase at 37°C in either the presence (std) or absence (no O_2) of oxygen. The levels of *cdr* were assayed in quadruplicate from three independently-derived samples by qRT-PCR and normalized to those of the *flaB* gene (84). Error bars indicate the standard error of the mean (SEM). The dagger (†) indicates significantly less *cdr* transcript in c162 grown under anaerobic conditions compared to the amount observed in c162 grown under standard conditions. The asterisk (*) denotes significantly less *cdr* in either c309 or c1655 relative to the levels observed in c162 grown under the same condition ($P < 0.05$).

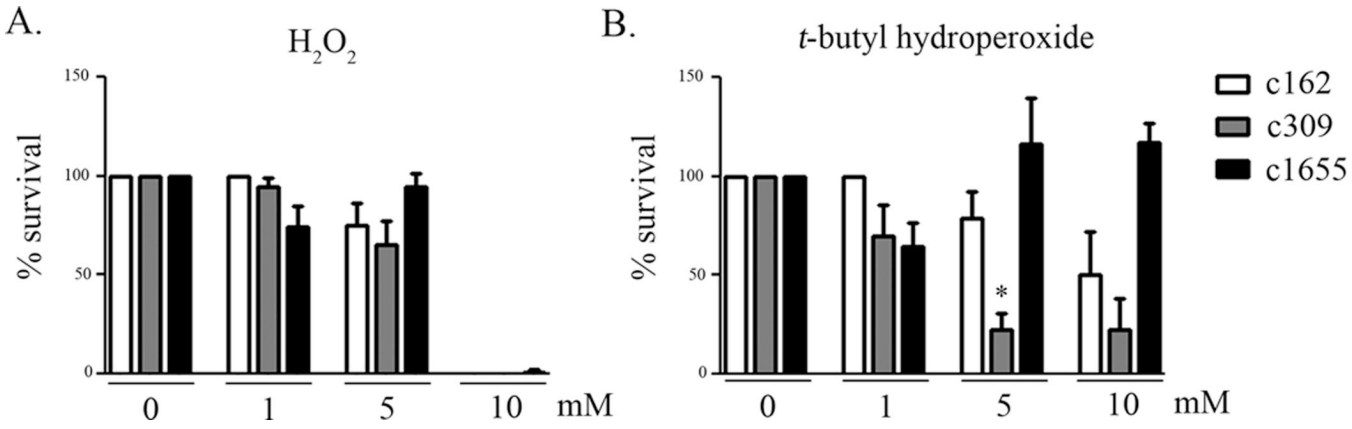

Figure 5.

Sensitivity of the *cdr* mutant to exogenous H_2O_2 or *t* -butyl hydroperoxide. c162 (wt), c309 (mut), and c1655 (ct) were exposed to the indicated concentration of (A) H_2O_2 or (B) *t*-butyl-hydroperoxide for 1 hr in media lacking BSA and rabbit serum. After exposure, the treated samples were diluted in fresh BSK-II and then serially-diluted 1:1 to 2.4×10^{-1} spirochetes per well. Wells were analyzed after three weeks for spirochetes. Results shown are the average of at least three replicates. Percentages are plotted relative to untreated sample of the same clone. Error bars indicate the SEM. The asterisk (*) indicates a significant difference between the mutant and wild-type clones.

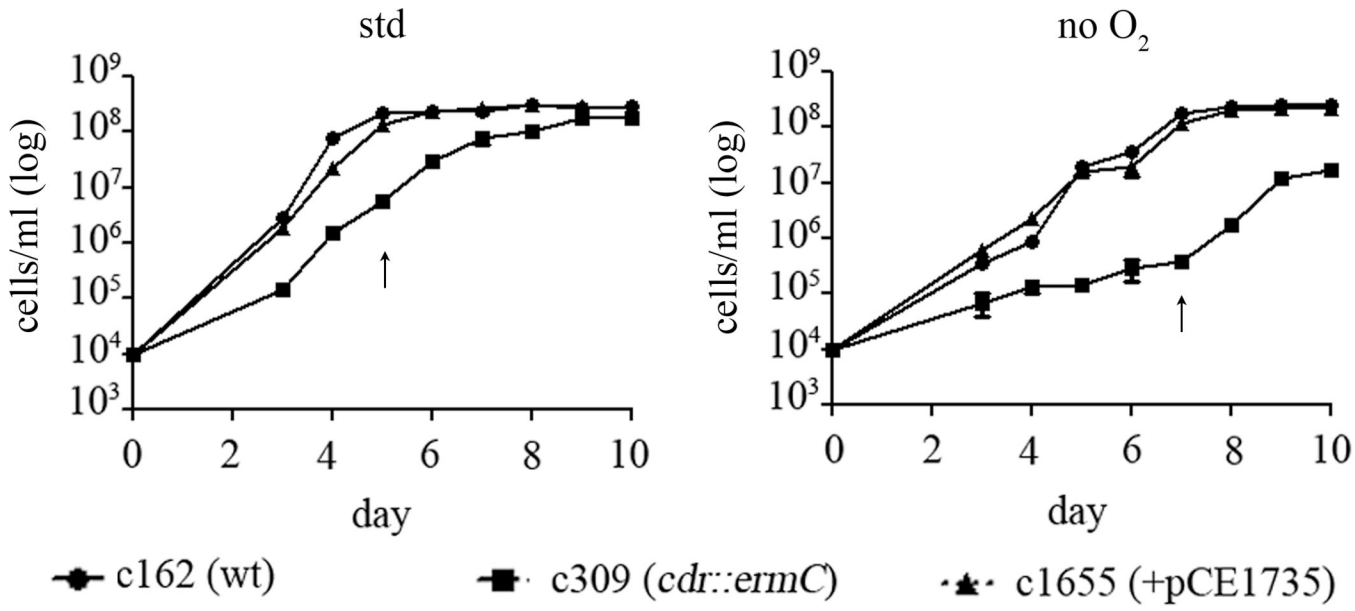

Figure 6.

The *cdr* mutant grown*in vitro* exhibits a growth defect that is even more severe during anaerobiasis. c162 (wt), c309 (mut), and c1655 (ct) were grown at 37°C under standard and anaerobic conditions. Density was measured daily using a Petroff-Hauser counting chamber. Each assay was done in triplicate and error bars represent the SEM. The point at which RNA samples were taken for Figure 4 is indicated by the arrows.

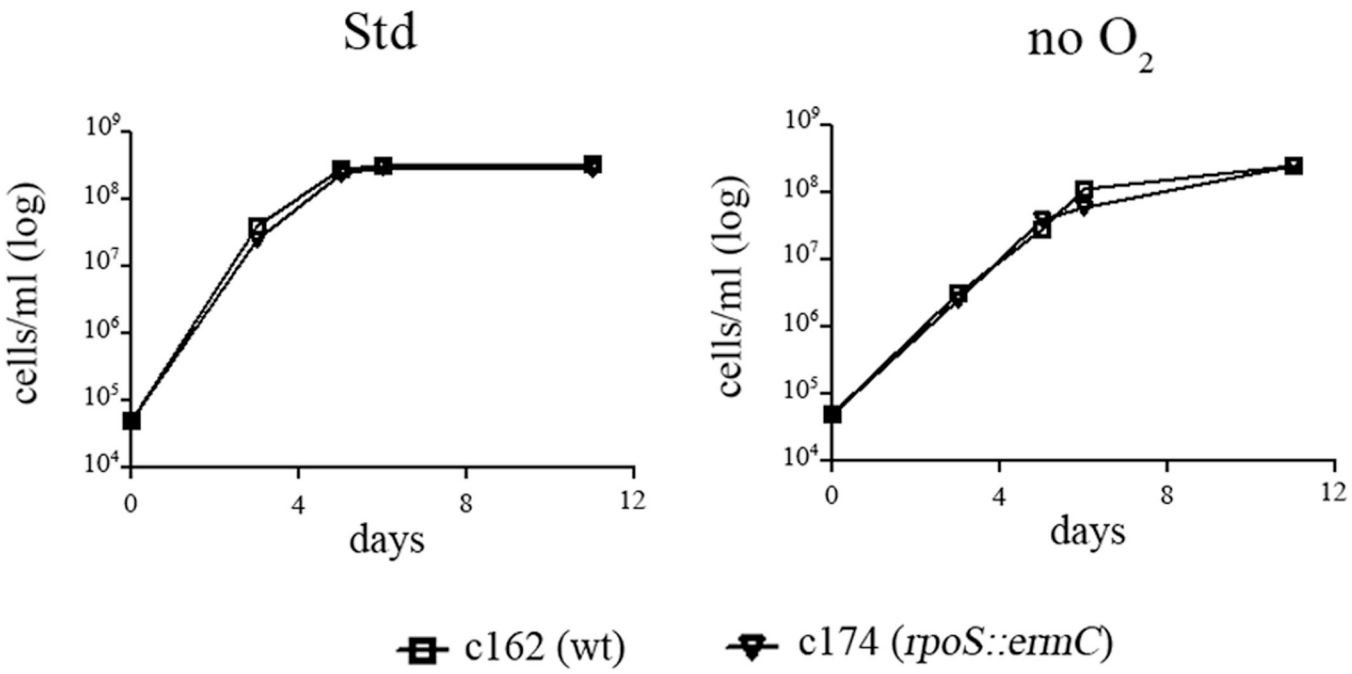

Figure 7.
An *rpoS* -mutant grown *in vitro* exhibits no growth defect. c162 (wt) and c174 (*rpoS* mutant) was grown at 37°C under standard and anaerobic conditions. Density was measured daily using a Petroff-Hauser counting chamber. Graphs shown are representative of three independent experiments.

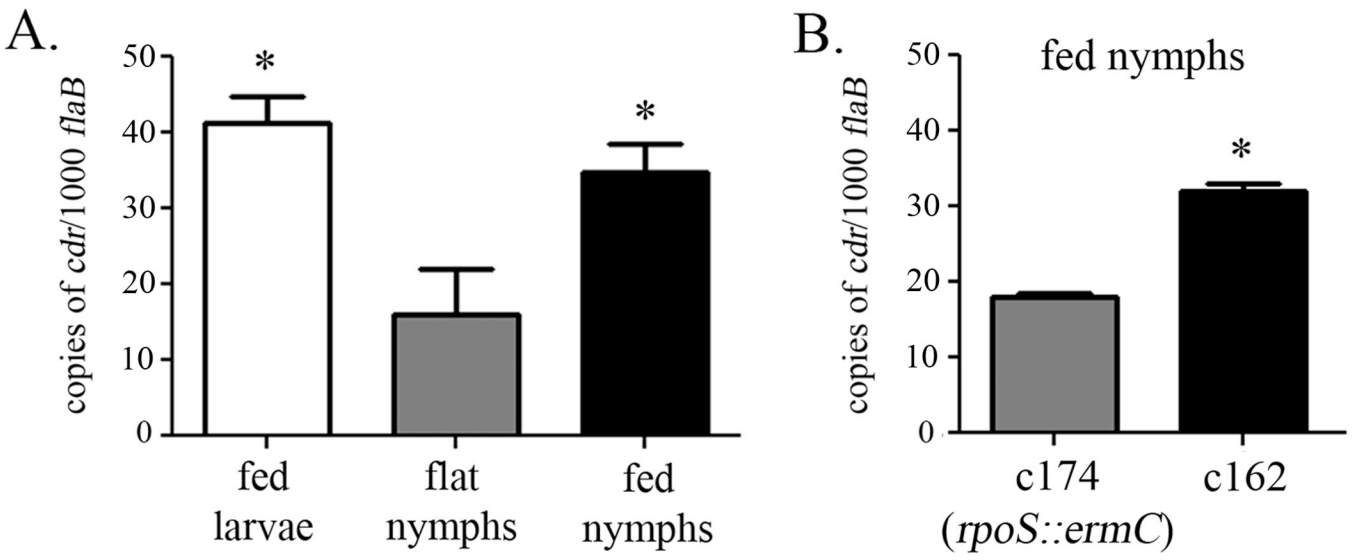

Figure 8.

Expression profiling analysis of *cdr* expression within ticks. (A) RNA was harvested from the midguts of c162-infected fed larvae, molted flat nymphs, and fed nymphs or (B) from the midguts of either c162- or c174-infected nymphs that had been fed on a mouse. The levels of *cdr* transcript in a pool of five ticks from each condition were analyzed in quadruplicate by qRT-PCR and normalized to those of the constitutively produced *flaB* gene (Ge *et al*., 1997). Error bars indicate the standard error of the mean (SEM). The asterisk (*) indicates significantly more *cdr* transcript ($P < 0.05$) in fed larvae and fed nymphs as compared to unfed flat nymphs(A), or in c162 within fed nymphs as compared to c174 within fed nymphs (B).

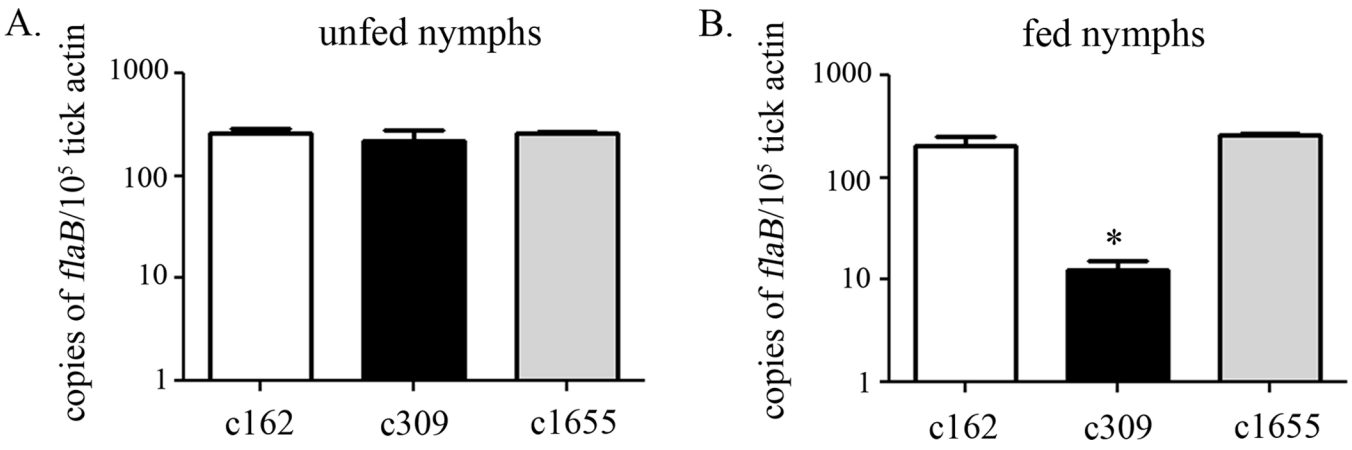

Figure 9.

Bb CoADR promotes survival of spirochetes within fed, but not flat, nymphs. *Ixodes scapularis* nymphs were rectally-infused with equivalent densities of wild-type (c162), *cdr* mutant (c309), and complemented (c1655) clones of *B. burgdorferi*. (A) After a ten day 'rest' period, relative *B. burgdorferi* burdens in unfed ticks were analyzed by qRT-PCR; the number of copies of the *B. burgdorferi flaB* transcript were normalized to tick β-*actin* RNA. The remainder of the rectally-infused nymphs were then allowed to feed upon SCID mice to repletion. (B) *B. burgdorferi* burdens in fed nymphs were monitored by qRT-PCR. The asterisk (*) denotes a significant difference between spirochetes in the midguts of fed nymphs infused with the *cdr* mutant compared to those infused with either the wild-type or the complement ($P < 0.05$). The data represent the average of four replicates of qRT-PCR analysis on two pools of three ticks (unfed) or 1–2 ticks (fed) from a representative experiment.

Table 1

B. burgdorferi clones used in this study

Clone name	genotype	Description	reference
c162	clone of strain 297	wild-type (wt)	(Caimano *et al*., 2007)
c309	c162 *cdr*::*ermC*	*cdr* mutant (mut)	This work
c1655	c309 + pCE1735 (*bb0729-cdr* operon); missing lp28-1	complement (ct)	This work
c174	c162 *rpoS*::*ermC*	*rpoS* mutant	(Caimano *et al*., 2004; Eggers *et al*., 2004)

Table 2

Oligonucleotides used in this study.

#[a]	Name	Sequence (5′-3′)	Description (reference)
1	*bb0729*-1225F	CTTTCCAGTGGGATTGGTAGGACTTG	mutant screening
2	*bb0728*-5′F (*Xho*I)[b]	GATCCTCGAGATGATGAAAATAATAATTATTGGGG	mutant generation
3	*bb0728*-3′R (*BamH*I)	GATCGGATCCTTCTTTCTATTTGGCAGCATTGCCAGC	mutant generation
4	*bb0727*-839F	CTTGATTTTGACATAGAAGGTCCTAATGG	mutant screening/ complement generataion
5	*ermC*-1F	CGATTCACAAAAAATAGGCACACG	mutant generation
6	*ermC*-464F	TCTTTGAAATCGGCTCAGGGGGGGGCC	mutant screening
7	*ermC*-808R	TCTGCCATTAAAAGTAATGCCAATGAGAGAGCG	mutant screening
8	*ermC*-1118R	AAACCGTGTGCTCTACGACCAAAAC	mutant generation/screening
9	*bb0730*-1159R (*Sph*I)	GATCGCATGCAGCTTGTAAACAAATAAATAGGAAAACA	complement generation
10	*bb0729*-550F-RT	GGCTTAGAAAAAACTCAACCATCG	RT-PCR
11	*bb0729*-805F-RT	GCTTCCTACATTGCCATAGGTCTTAC	RT-PCR
12	*bb0729*-1002R-RT	TTGCTATTCCTTCGCTTACTCC	RT-PCR
13	*bb0728*-140F-RT	TGGGGGGATTCTTTGACAAC	RT-PCR
14	*bb0728*-140R-RT	GTTGTCAAAGAATCCCCCCA	RT-PCR
15	*bb0728*-680F-RT	CTACTCCTTCTGCCTTTTTTTCTCC	RT-PCR
16	*bb0729*-GSP3	AAGGAGCCTTACGTATCCATCGC	5′-RACE
17	*bb0729*-GSP2	GTAGGCTCATTTTCCCAACATC	5′-RACE
18	*bb0729*-GSP1	CCTTCGGCTGTTAATCCCAATGC	5′-RACE
19	*bb0728*-GSP3	GTAAGGCAGGCCACAGGTTCC	5′-RACE
20	*bb0728*-GSP2	GATAACTTCGTGGTTAGTTTTAACAG	5′-RACE
21	*bb0728*-GSP1	GATTGGTGGAATAATAGGTTTTGCAC	5′-RACE
	bb0728-qRTPCR-R	GACGCTGTTATACTTGCTACCG	qRT-PCR
	bb0728-qRTPCR-R	GAAGCTGAGCCCAATGTGCCT	qRT-PCR
	bb0729-qRTPCR-F	TTGGGCGATGGATACGTAAGG	qRT-PCR
	bb0729-qRTPCR-F	CGCTTGTAGTCCTTCGGCTGT	qRT-PCR
	flaB-qRTPCR-F	CTTTTCTCTGGTGAGGGAGCTC	qRT-PCR and qPCR(Zhang *et al*., 2009)
	flaB-qRTPCR-R	GCTCCTTCCTGTTGAACACCC	qRT-PCR and qPCR(Zhang *et al*., 2009)
	flaB-probe	CTTGAACCGGTGCAGCCTGAGCA	qRT-PCR and qPCR(Zhang *et al*., 2009)
	nidogen-F	CCCCAGCCACAGAATACCAT	qPCR (Benhnia *et al*., 2005)
	nidogen-R	AAAGGCGCTACTGAGCCGA	qPCR (Benhnia *et al*., 2005)
	nidogen-Probe	CCGGAACCTTCCCACCCAGC	qPCR (Benhnia *et al*., 2005)
	Tick β-actin-F	GGTATCGTGCTCGACTC	qPCR(Zhang *et al*., 2009)
	Tick β-actin-R	ATCAGGTAGTCGGTCAGG	qPCR(Zhang *et al*., 2009)
	T7	TAATACGACTCACTATAGG	General screening
	M13R	GGAAACAGCTATGACCATG	General screening

[a] Corresponds to the primer number shown in Figure 2 (1–8) and Figure 3 (9–21).

[b] Restriction sites are underlined.

Table 3

Results of mouse infectivity studies.

Strain	exp	Mouse background	Seroconversion[a]	Culture positive	Visible arthritis[b]
C162 (wt)	1	C3H/HeJ	5/5	5/5	ND
	2	SCID	ND	4/4[c]	4/4
	3	SCID	ND	5/5	5/5
c309 (mut)	1	C3H/HeJ	0/5[d]	0/5	ND
(c162 *cdr*::*ermC*)	2	SCID	ND	0/5	0/5
	3	SCID	ND	0/5	0/5
c1655 (ct)	1	--[e]	--	--	--
(c309+pCE1735)	2	SCID	ND	5/5	4/5
	3	SCID	ND	5/5	5/5

[a] as determined by blotting *Bb* antigens with 8-wk mouse sera;

[b] observed 4 weeks after infection;

[c] one mouse died prior to evaluation;

[d] an immune response to only one antigen, OspC, was detected;

[e] the infection of C3H/HEJ mice with c1655 was not done (see text); ND, not determined

Table 4

Bioinformatics of genes involved in oxidative stress response and CoA biosynthesis in *B. burgdorferi*.

Protein	Functional homolog/PDB entry	Comparison or reference
Oxidative stress response[a]		
BB0728 (*cdr*)	CoADR/3CGC (*B. anthracis*)	40% identical, *E* value of 4×10^{-97} (Boylan *et al*., 2006)
BB0729 (*tcyP*)	Na^+/cystine symporter (*Bacillus subtilis*)	50% identical, *E* value of 6×10^{-111}
BB0515 (*trxB*)	thioredoxin reductase	(Fraser *et al*., 1997)
BB0061 (*trxA*)	thioredoxin	(Fraser *et al*., 1997)
BB0153 (*sodA*)	superoxide dismutase	(Esteve-Gassent *et al*., 2009)
BB0690 (*dps*)	Dps/NapA homolog	(Li *et al*., 2007)
Nox	NADH oxidase	None[b]
GshA	γ-Glu-Cys synthetase	None
GshB	GSH synthetase	None
GR	glutathione reductase	None
Grx	glutaredoxin	None
Gpx	glutathione peroxidase	None
AhpF	alkylhydroperoxide reductase	None
Prx	peroxiredoxin	None
CoA biosynthesis[c]		
BB0814 (*panF*)	Na^+/Pan symporter (*E. coli*)	34% identical, *E* value of 2×10^{-69}
BB0527 (*coaX; panK*)	Pan kinase/2H3G (*B. anthracis*)	28% identical, *E* value of 2×10^{-24}
BB0812 (*coaBC*)	phosphopantothenoylcysteine synthetase/1U7U (*E. coli*)	38% identical, *E* value of 2×10^{-27}
BB0702 (*coaD*)	phosphopantetheine adenylyltransferase/3F3M (*S. aureus*)	43% identical, *E* value of 1×10^{-28}
BB0547 (*coaE*)	dephospho-CoA kinase/1JJV (*Haemophilus influenza*)	30% identical, *E* value of 8×10^{-12}
BB0704 (*acpP*)	acyl carrier protein/2KWL	identical
PanB	ketopantoate hydroxymethyl-transferase	None
PanC	Pan synthetase	None
PanD	aspartate decarboxylase	None
PanE	2-dehydropantoate 2-reductase	None

[a] see also (Parsonage *et al*., 2010);

[b] None indicates that there has been no homolog identified within *B. burgdorferi*;

[c] see also (Boylan *et al*., 2006; Gherardini *et al*., 2010)